

VILNIUS UNIVERSITY
CENTER FOR PHYSICAL SCIENCES AND TECHNOLOGY

LEONA DAMALAKIENĖ (BANDZAITYTĖ)

FLUORESCENCE RESEARCH ON THE UPTAKE AND INTRACELLULAR
LOCALISATION OF COLLOIDAL QUANTUM DOTS AND THEIR EFFECT ON
MECHANISMS OF ENDOCYTOSIS

Summary of doctoral dissertation

Physical sciences, physics (02 P)

Vilnius, 2014

The study was carried out at Vilnius university during the period 2006 – 2013.

Scientific advisor:

Doc. dr. Saulius Bagdonas (Vilnius university, physical sciences, physics – 02 P).

Doctoral dissertation will be defended at Physical scientific board of Vilnius university:

Chairman:

Prof. dr. Roaldas Gadonas (Vilnius university, physical sciences – 02 P)

Members:

Prof. dr. Valdas Šablinskas (Vilnius university, physical sciences – 02 P)

Doc. dr. Mikas Vengris (Vilnius university, physical sciences – 02 P)

Prof. dr. Kęstutis Sužiedėlis (National cancer institute, physical sciences, biochemistry – 04 P)

Habil. dr. Vytenis Arvydas Skeberdis (Lithuanian university of health sciences, biomedical sciences, biophysics – 02 B)

Opponents:

Prof. dr. Saulius Šatkauskas (Vytautas Magnus university, biomedical sciences, biophysics – 02 B)

Dr. Dalia Kaškelytė (Vilnius university, physical sciences – 02 P)

Dissertation will be defended during the open session of Physical scientific board of Vilnius university on 9th of December, 2014 at 15.00 in auditorium 211, Faculty of physics of Vilnius university.

Address: Saulėtekio av. 9, III bld., LT–10222, Vilnius, Lithuania.

The summary of the doctoral dissertation has been sent on 7th of November 2014.

The dissertation is available in the Library of Vilnius university and Library of Center for physical sciences and technology.

.

VILNIAUS UNIVERSITETAS
FIZINIŲ IR TECHNOLOGIJOS MOKSLŲ CENTRAS

LEONA DAMALAKIENĖ (BANDZAITYTĖ)

KOLOIDINIŲ KVANTINIŲ TAŠKŲ KAUPIMOSI IR VIDULĄSTELINIO
PASISKIRSTYMO POVEIKIO ENDOCITIZACIJOS MECHANIZMAMS
FLUORESCENCINIAI TYRIMAI

Daktaro disertacijos santrauka

Fiziniai mokslai, fizika (02 P)

Vilnius, 2014

Disertacija rengta 2006 – 2013 metais Vilniaus universitete.

Mokslinis vadovas:

Doc. dr. Saulius Bagdonas (Vilniaus universitetas, fiziniai mokslai, fizika – 02 P).

Disertacija ginama Vilniaus universiteto Fizikos mokslo krypties taryboje:

Pirmininkas:

Prof. dr. Roaldas Gadonas (Vilniaus universitetas, fiziniai mokslai, fizika – 02 P)

Nariai:

Prof. dr. Valdas Šablinskas (Vilniaus universitetas, fiziniai mokslai, fizika – 02 P)

Doc. dr. Mikas Vengris (Vilniaus universitetas, fiziniai mokslai, fizika – 02 P)

Prof. dr. Kęstutis Sužiedėlis (Nacionalinis vėžio institutas, fiziniai mokslai, biochemija – 04 P)

Habil. dr. Vytenis Arvydas Skeberdis (Lietuvos sveikatos mokslų universitetas, biomedicinos mokslai, biofizika – 02 B)

Oponentai:

Prof. dr. Saulius Šatkauskas (Vytauto Didžiojo universitetas, biomedicinos mokslai, biofizika – 02 B)

Dr. Dalia Kaškelytė (Vilniaus universitetas, fiziniai mokslai, fizika – 02 P)

Disertacija bus ginama viešame Fizikos mokslo krypties tarybos posėdyje 2014 m. gruodžio mėn. 9 d., 15 val., Vilniaus universiteto Fizikos fakulteto 211 auditorijoje.
Adresas: Saulėtekio al. 9, III-ieji rūmai, LT–10222 Vilnius, Lietuva.

Disertacijos santrauka išsiuntinėta 2014 m. lapkričio mėn. 7 d.

Disertaciją galima peržiūrėti Vilniaus universiteto ir Fizinių ir technologijos mokslų centro bibliotekose.

Table of Contents

Abbreviations	7
1 Introduction	8
1.1 Relevance.....	8
1.2 Objectives of the study	10
1.3 Statements to be defended	10
1.4 Scientific novelty	11
2 Materials and methods.....	13
2.1 Cell cultures	13
2.2 Quantum dots and other chemicals.....	13
2.3 Photoluminescence spectroscopy	14
2.4 Confocal microscopy	15
2.5 Fluorescence lifetime imaging microscopy.....	15
2.6 Microinjection.....	16
2.7 Transfection with Green Fluorescent Protein plasmid	16
3 Results and discussion	17
3.1 Intracellular accumulation and distribution of quantum dots.....	17
3.2 Uptake mechanism of quantum dots	23
3.3 Overview of the process and mechanism of quantum dots' intracellular uptake	
32	
3.4 Precautions for the combined application of QDs and biomedical agents.....	35
4 Conclusions	39
5 References	40
6 Santrauka	46
6.1 Aktualumas	46
6.2 Tyrimų tikslas ir uždaviniai	48

6.3	Ginamieji teiginiai	48
6.4	Naujumas	49
6.5	Pagrindiniai rezultatai	50
6.6	Išvados	52
7	List of publications	54
8	CURRICULUM VITAE	55

Abbreviations

Ce ₆	–	chlorin e6
DexB	–	dextran
EGFP	–	enhanced green fluorescent protein plasmid
FLIM	–	fluorescence lifetime imaging microscopy
HepG2	–	human hepatocellular carcinoma-derived cell line
LacCer	–	lactosylceramide
LDL	–	low-density lipoprotein
LE	–	late endosome
LYS	–	lysosome
MCF-7	–	human breast adenocarcinoma cell line
NDD	–	nanoparticle-based drug delivery
NIH3T3	–	immortalized mouse embryonic fibroblast cell line
PL	–	photoluminescence
QD(s)	–	quantum dot(s)
QD625	–	quantum dots with a photoluminescence peak at 625 nm
QD545	–	quantum dots with a photoluminescence peak at 545 nm
QD-saturated cells	–	The cells incubated with QDs until the saturation phase
Trf	–	transferrin

1 Introduction

1.1 Relevance

The application of nanotechnology to medicine and introduction of nanomaterials in drug formulation strategies (defined as nanomedicine¹) became sources of major innovations in drug delivery over the last decade,^[1] dedicated to achieve maximal effectiveness against the existing disease and as minimal side effects (effects on non-targeted tissues) as possible, and are considered to be highly useful for personalizing nanomedicine-based (chemo-) therapeutic interventions.^[2] The premiere advantage of nanocarriers is their potential for multi-functionality, which enables accommodation of diagnostic and therapeutic materials such as drugs, affinity ligands, and imaging moieties within a single nanoparticle vector to achieve targeted and traceable drug delivery. Any colloidal object (organic and inorganic particles, vesicles, liposomes, micelles and soluble macromolecules) of size from several nanometres to few micrometres could be used as a nanocarrier. Recently, there has been an explosion in the development of nanocarrier vehicles composed of lipids, polymers, carbon materials, inorganic nanocrystals, and even hybrid combinations of those materials^[3] tailored towards not only dramatically improving pharmacologic properties of existing therapeutics,^[4] but also enabling delivery of new classes of potent anti-cancer drugs for gene therapy and immunotherapy.^[5]

Nanoparticle-based drug delivery (NDD) has emerged as a promising approach to improve the efficacy of existing drugs and enable the development of new therapies. Proof-of-concept studies have demonstrated the potential for NDD systems to simultaneously achieve reduced drug toxicity, improved bio-availability, increased circulation times, controlled drug release, and targeting. However, clinical translation of NDD vehicles with the goal of treating particularly challenging diseases, such as cancer, will require a thorough understanding of how nanoparticle physicochemical properties influence their fate in biological systems, *in vitro* and *in vivo*. Consequently, a model system for systematic evaluation of all stages of NDD with high sensitivity, high

¹Nanomedicine aims at ensuring the comprehensive monitoring, control, construction, repair, defence and improvement of all human biological systems, working from the molecular level using engineered devices and nanostructures, ultimately to achieve medical benefit.

resolution, enabling functionalization and low cost is highly desirable. In theory, this system should maintain the properties and behaviour of the original NDD vehicle, while providing mechanisms for monitoring intracellular and systemic nanocarrier distribution, degradation, drug release, and clearance. For such a model system, semiconductor nanocrystals – quantum dots (QDs), due to their unique physical, chemical and optical properties, offer great potential^[6] for research how to control the properties of designed nanocarriers. QDs provide a perspective towards the notable potential application of their use as therapeutic and diagnostic tools in nanomedicine,^[7] for example site-specific medical imaging and drug delivery, or in cancer treatment.^[8] Together with the main benefits, such as localization of QDs within cells at subcellular resolution, sensitivity to microenvironment, a narrow emission profile and a large Stokes shift, which are actual for QDs optical imaging, QDs feature a small size and versatile surface chemistry and offer superb optical properties – high brightness and high photostability, – for real-time monitoring of NDD vehicle transport and drug release at both cellular and systemic levels.^[9] Though the nanocrystals of QDs are commonly composed of toxic materials (such as cadmium, Cd), QDs with the surface coating and passivation do not induce acute toxicity *in vitro* and *in vivo*.^[10,11] The properties of QDs enabled them to be extensively used as a nanocarrier model for the study of many steps of the nanoparticle-based drug delivery, including critical mechanisms of intracellular uptake and trafficking as well as overall *in vivo* biodistribution, in order to define a set of design parameters that could lead further engineering efforts in NDD. In the long-term, the QDs core can be replaced with other nanoparticle of interest (such as gold and magnetic nanoparticles, potentially providing additional therapeutic functionalities) without interference with predefined fate in biological systems.^[12]

Current progress in the synthesis of biocompatible QDs has made it possible to produce a large variety of semiconductor nanocrystals in terms of size, surface functionality, bioconjugation and targeting. For all types of nanoparticles, the features of the nanoparticle surface, such as its size, shape, charge and chemical functionality (coating/design), are still considered to be extremely important to its biological interactions because changes in its surface properties significantly alter its uptake, localization and fate.^[12,13] Therefore, it is essential to confirm the feasibility of cellular uptake and to understand and quantitate the internalization rate and the intracellular fate

of nanoparticles, as these issues are the key factors that determine the clinical efficacy of NDD.^[14] Many studies aiming to correlate the above mentioned properties of QDs with biomolecular signalling, biological kinetics, transportation and toxicity have been performed on cell cultures and experimental animals.^[7, 15-18] However, it is difficult to compare and draw an unambiguous conclusion from the reports on studies available to date because they included a variety of QDs, cell lines and analytical methods. Moreover, many of the conclusions drawn about cellular uptake of nanoparticles need to be re-evaluated in light of the present knowledge of endocytic mechanisms and their influence on the fate of nanoparticles.^[19] Therefore, expanding of the understanding about nanoparticle uptake, intracellular localization and transportation consistency would enable the more precise interpretation of *in vitro* research results and would facilitate the development of *in vivo* applications for nanoparticles.

1.2 Objectives of the study

The overall aim of the study is to identify the general rules for intracellular uptake and localisation of non-targeted nanoparticles by employing colloid quantum dots as a model of biocompatible nanoparticle-based drug carriers.

The following specific objectives were formulated:

1. To determine the accumulation dynamics of quantum dots in normal and cancer cell lines by means of spectroscopic methods.
2. To investigate the intracellular localisation of quantum dots by using the confocal fluorescence microscopy and fluorescence lifetime imaging microscopy methods.
3. To determine the uptake pathways of the quantum dots and the influence factors for the pathways.
4. To evaluate the influence of quantum dots on the cells when being applied as diagnostic particles for combined therapy.

1.3 Statements to be defended

1. The uptake process of non-targeted negatively charged quantum dots can be divided into three time related accumulation stages: I – a plateau stage, II – a growth stage and III – a saturation stage, which are characteristic for all

investigated cell lines, but the stages were of different timing for each of the cell line. The accumulation of quantum dots can be divided according to the intracellular distribution and the types of formed vesicles by four phases: phase 1 – adherence to the cell membrane; phase 2 – formation of granulated clusters spread in the cytoplasm; phase 3– localization of granulated clusters in a perinuclear region; and phase 4 – formation of multi-vesicular bodies and their redistribution in the cytoplasm.

2. QD-filled endosomes mature in time with increasing inner heterogeneity, which characterised by growing down photoluminescence lifetime of accumulated QDs.
3. Quantum dots do not penetrate the plasma and inner membranes of cells through passive diffusion.
4. Quantum dots, incubated with fibroblast cells (NIH3T3) in a serum-free medium, enter the cells through the only caveolin-dependent endocytic pathway, which could be suppressed and restored afterwards.
5. The intracellular accumulation of quantum dots potentially has effect on uptake of drug substances and on increment of cell drug-resistance.

1.4 Scientific novelty

During this study the consistent studies of the intracellular uptake of purposely non-targeted negatively charged quantum dots (QDs) were carried out. The accumulation and the intracellular distribution of QDs were investigated, the structure of QDs-filled intracellular vesicles were analysed and the uptake mechanism of QDs was determined.

The time related intracellular accumulation stages of QDs: I – a plateau stage ($t_{inc} < 0,5$ h); II – growth (t_{inc} 0,5-6) h and III – a saturation stage ($t_{inc} > 6$ h) and the intracellular localisation phases: 1 – adherence to the cell membrane (t_{inc} 0.5-1 h); 2 – formation of granulated clusters spread in the cytoplasm (t_{inc} 0.5-6 h); 3– localization of granulated clusters in a perinuclear region (t_{inc} 6-24 h); and phase 4 – formation of multi-vesicular body-like structures and their redistribution in the cytoplasm were investigated in the long-term and described for the first time. Moreover, the possibility to identify the maturity of endosomes filled with quantum dots and to image their sub-structure by using fluorescence lifetime imaging microscopy technique was firstly demonstrated.

The microinjection of the suspension of QDs into the live cells, imitating the passive diffusion through the plasma membrane has been performed. After comparative analysis of QDs accumulation in cells transfected with enhanced green fluorescent protein plasmid (EGFP) it was demonstrated that the passive transfer of QDs through the plasma and inner membranes of cells is restricted.

It was determined that the uptake of the purposely non-targeted negatively charged QDs into NIH3T3 cells occurs via caveolin depended endocytic pathway. For the first time it was demonstrated that the saturating accumulation of QDs affects the intracellular localisation of caveolin-1, the molecule required for invagination of plasma membrane and formation of caveolae, its distribution and accumulation in QDs-filled vesicles.

Moreover, the increased resistance of the cells pre-incubated with the QDs to the chemotoxicity of cisplatin has been demonstrated. That result should be taken into account in the future development of QDs and other nanoparticles as diagnostic and therapy probes.

2 Materials and methods

2.1 Cell cultures

An immortalized mouse embryonic fibroblast cell line NIH3T3, a human breast adenocarcinoma cell line MCF-7 and a human hepatocellular carcinoma-derived cell line HepG2 have been cultured in the presence of CO₂ (5 % v/v) at 37°C in Dulbecco's Modified Eagle's Medium (DMEM, Gibco, USA) supplemented with fetal bovine serum (10 % v/v), 0.1 % antibiotics (stock: 1000 U/ml Penicillin, 1000 µg/ml Streptomycin) to get ~60 % of confluence.

To evaluate the uptake dynamics and intracellular localization of the QDs, cells were seeded at a density of 40% confluence in DME medium, in either 24-well plates for PL spectroscopy or 8-well chambered cover-slips (Nunc, USA) for microscopy, and allowed to grow for 24 h until they reached ~70% confluence. Prior to all experiments, the cells were rinsed three times with DME medium and left for 2 h in serum-free DME medium at 37 °C.

The final 10 nM concentration of QDs was used in the incubation medium for all experiments.

2.2 Quantum dots and other chemicals

The carboxyl-functionalized quantum dots (QDs) used in this study (eFluor™ 625NC and 545NC) were purchased from eBioscience™ (USA). These QDs show photoluminescence (PL) peaks at 625 nm (QD625) and 545 nm (QD545), have an identical structure (a CdSe core passivated with a ZnS shell) and are capped with a micelle-like coating of amphiphilic 1,2- distearoyl-*sn*-glycero-3-phosphoethanolamine-*N*-[carboxy(polyethylene glycol)-2000], i.e., DSPE-PEG2000 functionalized with carboxyl groups.

AlexaFluor®488-conjugated transferrin (Trf), BODIPY₅-lactosylceramide/BSA (LacCer) and DextranCascade Blue (DexB) were purchased from Invitrogen (USA). The photosensitizer chlorin e6 (Ce₆) was purchased from Frontier Scientific Inc. (USA). Cisplatin was purchased from Teva Pharma B. V. (Holland) and used at 0.075 µg/mL or 0.5 µg/mL for 24 h. The expression vector pEGFP-C1-Caveolin-1 (dog Caveolin-1 fused to enhanced green fluorescent protein) was a gift from Lisette Leyton.^[20]

2.3 Photoluminescence spectroscopy

The cells were seeded in 24-well plates for 24 h in FBS-free medium and then incubated with carboxylated QDs in FBS-free medium over a time course ranging from 15 min to 48 h (37 °C, 5% CO₂). After the indicated time of incubation, the cells were rinsed three times with PBS and detached from the plates with trypsin. Then, the cells were collected and re-suspended in PBS to a final volume of 1.5 mL. The cell number was counted with a hemocytometer. Quantitative analysis of the intracellular uptake of the QDs into living cells was performed with a steady-state and fluorescence lifetime spectrometer (FLS920; Edinburgh Instruments, UK), recording the mean PL signal of the accumulated QDs, which was normalized per cell. Each cell suspension was placed in a 1-cm-pathlength plastic cuvette (Hellma Optics, Germany). The temperature of the sample was maintained at 37 °C while the cell suspension was constantly stirred to sustain its homogeneity. The PL excitation wavelength was set to 405 nm, and the excitation and emission slits were kept at 5 nm. The PL spectra of the QDs and the fluorescence spectra of the endocytosis reporters and dyes in each sample were repeatedly measured three times. The autofluorescence of the cell suspension was also measured in control samples and considered in the data analysis. NIH3T3 cells were pretreated for 24 h with either 10 nM QD545 to study the subsequent internalization of QD625, DexB and Ce₆, or with 10 nM QD625 to study the uptake of LacCer and Trf at different incubation times ranging from 1 h to 24 h. Prior to the secondary incubation, the cells were rinsed three times with FBS-free medium to prevent co-incubation of the QDs and the agents under investigation.

To determine the duration of the suppression of QD uptake, the cells were pretreated with QD625 for 24 h, rinsed three times and kept in FBS-free medium without QDs for 2, 5 or 7 h. After the indicated time, a new dose of QDs was infused into the medium, and the cells were further incubated for 1 h. Then, the cells were prepared for determination of their PL signal using the procedures described above. Two PL experiments were performed in parallel: one batch of pretreated and rinsed cells was kept in DME medium without QDs and the other batch was kept in medium supplemented with the same QD625.

Data are presented as the mean values of at least three independent experiments \pm SE. Statistical analysis was performed using one-way ANOVA, and differences were considered significant at $p < 0.05$.

2.4 Confocal microscopy

Living cells were incubated in serum-free media for different periods and then imaged with a confocal microscope (Nikon Eclipse TE2000-S, C1 plus) by sequential scanning with a beam of an Argon ion laser (488 nm), at 600X total magnification using a 60X NA 1.4 objective (Plan Apo VC, Nikon, Japan). For standard images the three-channel RGB detector (band-pass filters: 515/30 and 605/75 for green and red channel, respectively) was used. Image processing was performed using the “Nikon EZ-C1 Bronze version 3.80” and “ImageJ 1.41” software. The QDs imaging in a red (R) spectral range (578-632 nm) was done retaining the same parameters for all fluorescence images. All cell lines were rinsed 3 times with a warm DME medium before imaging.

2.5 Fluorescence lifetime imaging microscopy

Fluorescence lifetime images were acquired using Lifetime and FCS Upgrade for Nikon C1si (PicoQuant GmbH, Germany). The system consisted of a 405 nm pulsed diode laser with a pulse width of 39 ps and a repetition rate of 10 MHz, which allowed using a measurement time interval of 100 ns. Detected photons were counted by a time correlated single-photon counter PicoHarp 300 (PicoQuant GmbH, Germany). Initialization, scanning, and acquisition were controlled by the same Nikon C1si microscope system. PL lifetime signal of QDs in living cells was detected with a single channel unit of single photon counting avalanche photodiodes (SPADs) at a spectral range of 578 ± 52.5 nm. Each lifetime image was obtained by collecting 1000 counts at the peak value, and the image resolution was fixed at 512x512 pixels. Fluorescence lifetime imaging microscopy (FLIM) images were reconstructed using a three-exponential fitting model (SymPhoTime software, PicoQuant GmbH, Germany), in which an average lifetime of QDs is displayed for every given pixel. Histograms for all average lifetimes (for all pixels) of QDs were plotted using the SymPhoTime v.5.2 (PicoQuant GmbH, Berlin, Germany) software.

2.6 Microinjection

The injection solution was prepared diluting 0.5 μl of QDs from a stock solution in 9.5 μl of PBS. A microinjector (Eppendorf FemtoJet and CellTram Air; Hamburg, Germany) was used for direct injection of QDs into the cytoplasm (the injection pressure – 200 hPa; the rate – 500 $\mu\text{m/s}$). The confocal fluorescence images of the cells were taken immediately after the injection and after incubation for 24 h (37°C, 5% CO₂).

2.7 Transfection with Green Fluorescent Protein plasmid

Temporal transfection of NIH3T3 with a EGFP plasmid followed the standard protocol for transfection of adherent cells. The following solutions were prepared separately: *Solution A*: the eGFP plasmid in 50 μl of DME medium; *Solution B*: 1.5 μg of MetafectenePRO (Biontex) in 50 μl of DME medium free of antibiotics. Mixed solutions were kept at room temperature for 20 min. The formed plasmid-MerafectenePRO complexes were added to the plates with NIH3T3 cells. After 6 h the transfection mixture was removed and replaced with the fresh DME medium supplemented with a fetal bovine serum (10 % v/v), 0.1 % antibiotics (stock: 1000 U/ml Penicillin, 1000 $\mu\text{g/ml}$ Streptomycin) and the plates were returned to the CO₂ incubator and were kept until the time of experiments.

Transient transfection of NIH3T3 cells with EGFP-C1-Caveolin-1 plasmid was performed using TurboFect transfection reagent according to manufacturer's recommendations (Thermo Fisher Scientific Inc., Lithuania). Briefly, the cells were grown in complete DME medium (37 °C, 5% CO₂ up to ~50% confluence) and then transfected for 24–48 h using TurboFect transfection reagent with the corresponding plasmid followed by subsequent analysis as indicated.

3 Results and discussion

3.1 Intracellular accumulation and distribution of quantum dots

The uptake kinetics drawn on the basis of the changes of the red photoluminescence (PL) intensity revealed a “S”-shaped (a plateau stage, a growth stage and a saturation stage) time dependence for the accumulation of carboxyl-QDs in different cell lines (NIH3T3, HepG2 and MCF-7) during incubation at 37°C: (Figure 1, A), but the stages were of different timing for each of the cell lines (Figure 1, B). The PL intensity of carboxyl-coated QDs incubated with NIH3T3 and MCF-7 cells increased with time and started to saturate after 6 h. The PL intensity in the case of HepG2 cells remained very weak and started to grow only after 30 h. The confocal fluorescence images taken instantly, 0.5 h, 1 h, 6 h, 24 h and 48 h after the incubation of cells with QDs (Figure 1, C-F) showed the evolution of the distribution pattern and the transport vesicles of carboxyl-coated QDs in the cells: phase 1 – adherence to the cell membrane (t_{inc} 0.5-1 h) (Figure 1, C); phase 2 – formation of granulated clusters spread in the cytoplasm (t_{inc} 0.5-6 h) (Figure 1, D); phase 3– localization of granulated clusters in a perinuclear region (t_{inc} 6-24 h) (Figure 1, E); and phase 4 – formation of multi-vesicular body-like structures and their redistribution in the cytoplasm ($t_{\text{inc}} > 24$ h) (Figure 1, F). The granulated pattern of the red PL of QDs present inside the NIH3T3 cells (assigned to the phase 2, Figure 1, D), indicated that QDs were trapped in vesicular structures. The QDs remained inside vesicles during a whole period of observation, only the number of vesicles per cell increased during the phases 3 and 4 (Figure 1 E, F and Figure 1 B-D), as did their size and PL intensity.

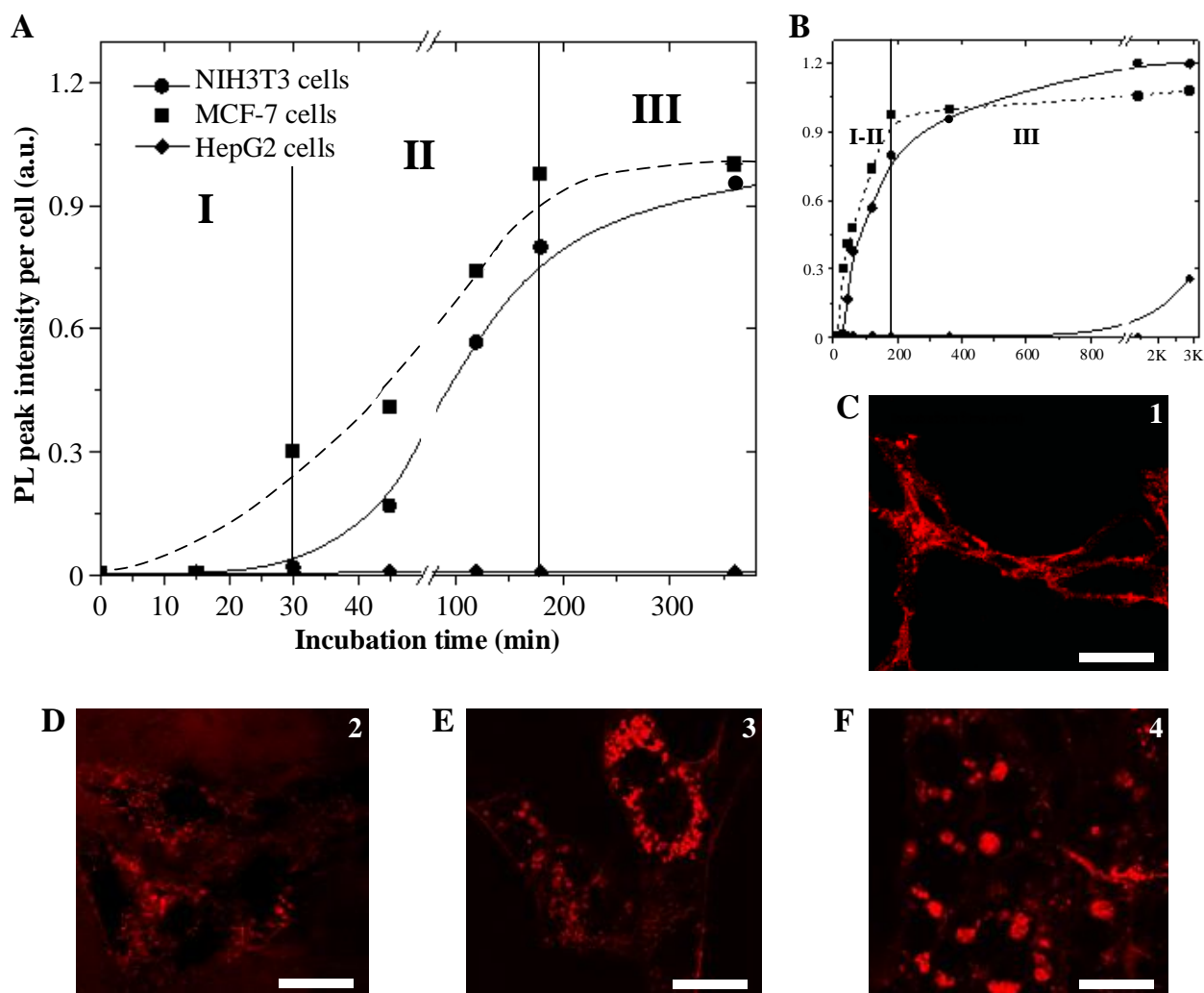


Figure 1: A, B – internalization dynamics of carboxy-QDs into NIH3T3, HpG2, MCF-7 cells at 37°C with indicated stages of accumulation presented in different scale range, accompanied with confocal fluorescence images of NIH3T3 cells illustrating the observed accumulation phases (C – phase 1: adherence to cell membrane; D – phase 2: formation of vesicular structures spread in the cytoplasm; E – phase 3: vesicle fusion and localization in the perinuclear region; F – phase 4: formation of the multi-vesicular bodies- like structures and their redistribution in the cytoplasm). Serum-free medium, scale bar 20 μm

Diverse vesicles ranging from $\sim 0.5 \mu\text{m}$ to $8 \mu\text{m}$ in diameter (Figure 2) have been observed on close inspection. The fluorescence images of the smallest vesicles with a diameter up to $0.5 \mu\text{m}$ were detected during the phase 2 (Figure 2, A). Two different vesicle types of the same size ($\sim 1 \mu\text{m}$ in diameter) were observed during the phase 3: those fully filled with QDs (Figure 2, B) and the ring-like vesicles with QDs being attached to the inner surface without distribution throughout the volume (Figure 2, C). The largest vesicles ($\sim 5\text{-}8 \mu\text{m}$) that were observed during the phase 4 revealed to be

multi-vesicular bodies^[21] being formed of many small vesicles that were fully filled with QDs and were packed into a single large vesicle (Figure 2, D).

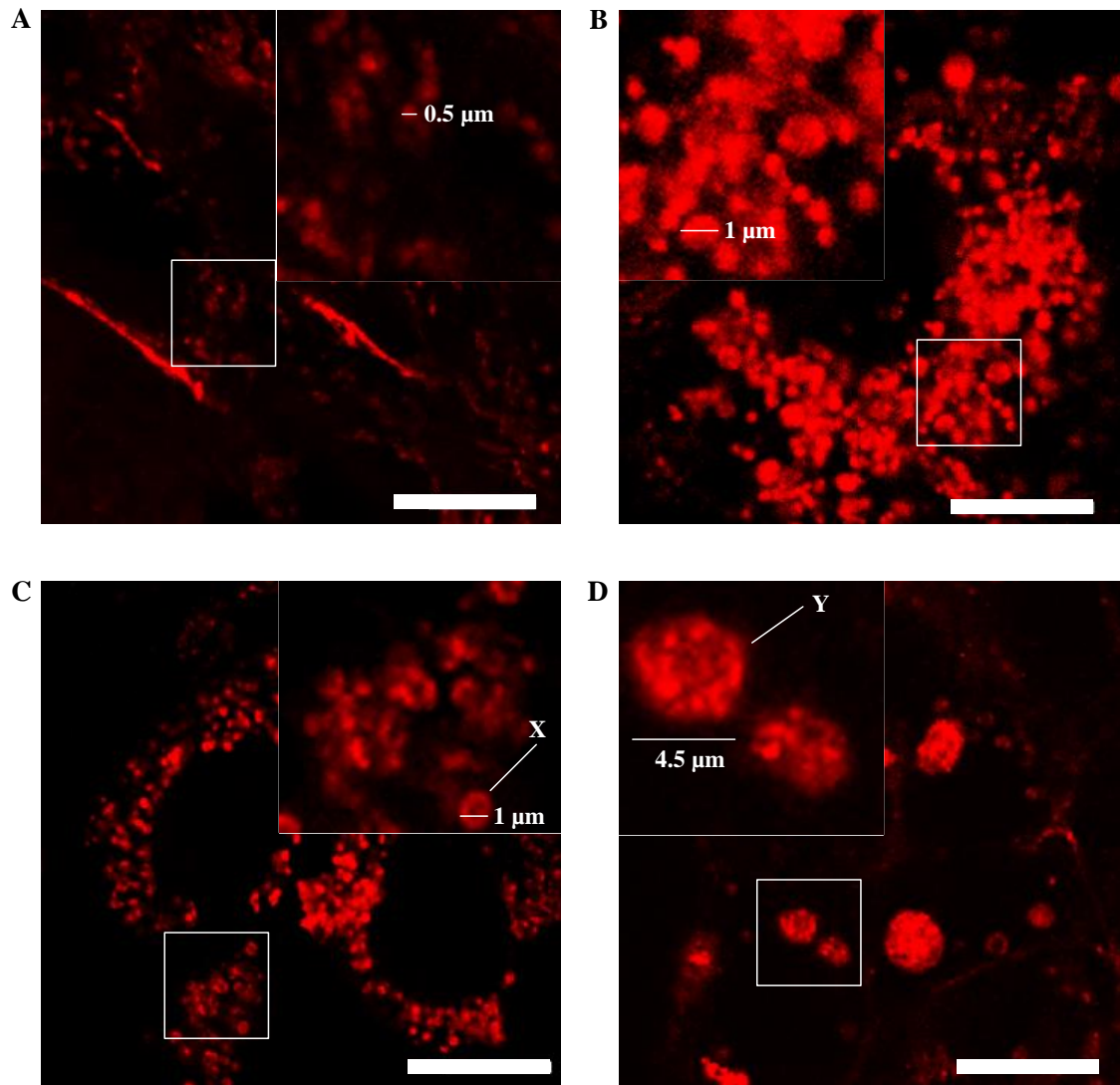


Figure 2: Confocal fluorescence images of types of vesicular structures formed in NIH3T3 cells during phase 2 (A), phase 3 (B, C) and phase 4 (D) of incubation with QDs. X – ring like images of vesicles with QDs attached to the inner surface of vesicle without distribution throughout the volume; Y – large vesicles, multi-vesicular bodies-like structures. Scale bar 10 μm

The QDs uptake process begins with their adherence to receptors on cell surface that are present in plasma membrane. Following the energy dependent internalization during the phase 1 this complex then enters the cells in the form of cargo located inside receptor-coated vesicles called endocytic vesicles. At the phase 2, endocytosed cargo is usually delivered to the early endosomes.^[22] This process is followed by their controlled migration (against a concentration gradient), fusion and localization in the perinuclear

region (phase 3), close to the Golgi complex and microtubule organizing centre.^[23] According to observed sizes and structure the QD-containing vesicles could be categorized into three groups: (i) vesicles up to 1 μm in diameter, formation time 15 min – 1 h, which could be assigned to endocytic vesicles that merge into larger vesicles by homotypic fusion;^[24] (ii) vesicles up to 5 μm in diameter, formation time beyond 1 h, referred as early endosomes, which are mainly spherical^[25] and (iii) vesicles more than 5 μm with the presence of intraluminal vesicles, referred as late endosomes / multi-vesicular bodies.^[26] Despite of time-related differences, the distribution of non-targeted QDs followed the similar accumulation stages and phases in different cell lines (NIH3T3, HepG2 and MCF-7). We would like to mention that the phases of accumulation of QDs were not equally clearly expressed in the studied cell lines. The main reasons could be the different physiology of cell lines and cell type-specific surface receptors.^[27] The observed variations in uptake timing between the cell lines (Figure 1, A-B) may also be influenced by the cell-related differences in internalization mechanisms of QDs. It should be noted that similar distribution of QDs in the cells, which is we have attributed to phases 1 and 2, were presented earlier in studies of A. Hoshino et al.,^[28] M.J.D. Clift et al.^[29] and W. Jiang et al.^[30] T.A. Kelf et al.^[31] Y. Williams et al.^[32] and F. Corsi et al.^[33] have shown the formation of vesicular structures spread in the cytoplasm corresponding to the phase 2. The phase 3 – the localization of vesicular structures in the perinuclear region – was described by L.W. Zhang et al.,^[34] Y. Xiao et al.^[35] and reviewed by W.J. Parak^[36] The phase 4 resembles the data about the formation of multi-vesicular body-like structures and their redistribution in cytoplasm, presented by Y. Yuan et al.^[39] and W. Jiang et al.^[30] However, there the accumulation phases of QDs was not introduced and there was no presentation of an overall picture illustrating the time-dependent manner of natural uptake and distribution of non-targeted negatively charged QDs in living cells.

Fluorescence lifetime imaging microscopy (FLIM) images taken at three defined time-gates enabled to register the spatial heterogeneity of the intracellular vesicles. The differences in fluorescence lifetimes were employed to monitor the intracellular trafficking of QDs in detail through all previously demonstrated stages of intracellular accumulation (Figure 3). After 1 h to 3 h of incubation (when QDs are either adherent to the membrane, or are in the small – up to 1 μm in diameter – endocytic vesicles

distributed in cytoplasm) the photoluminescence (PL) lifetimes are mainly in the range of 16-22 ns. After longer (< 6 h) incubation, when larger endosomes (~2-3 μm in diameter) with QD are concentrated in a perinuclear region – an additional range of shorter PL lifetimes (10-15 ns) was registered. And for the cells being in the saturation stage – after incubation of 24 h, when the multi-vesicular bodies (~3-8 μm) are formed and distributed in the cytoplasm – the increased input of even shorter (5-9 ns) PL lifetimes was detected.

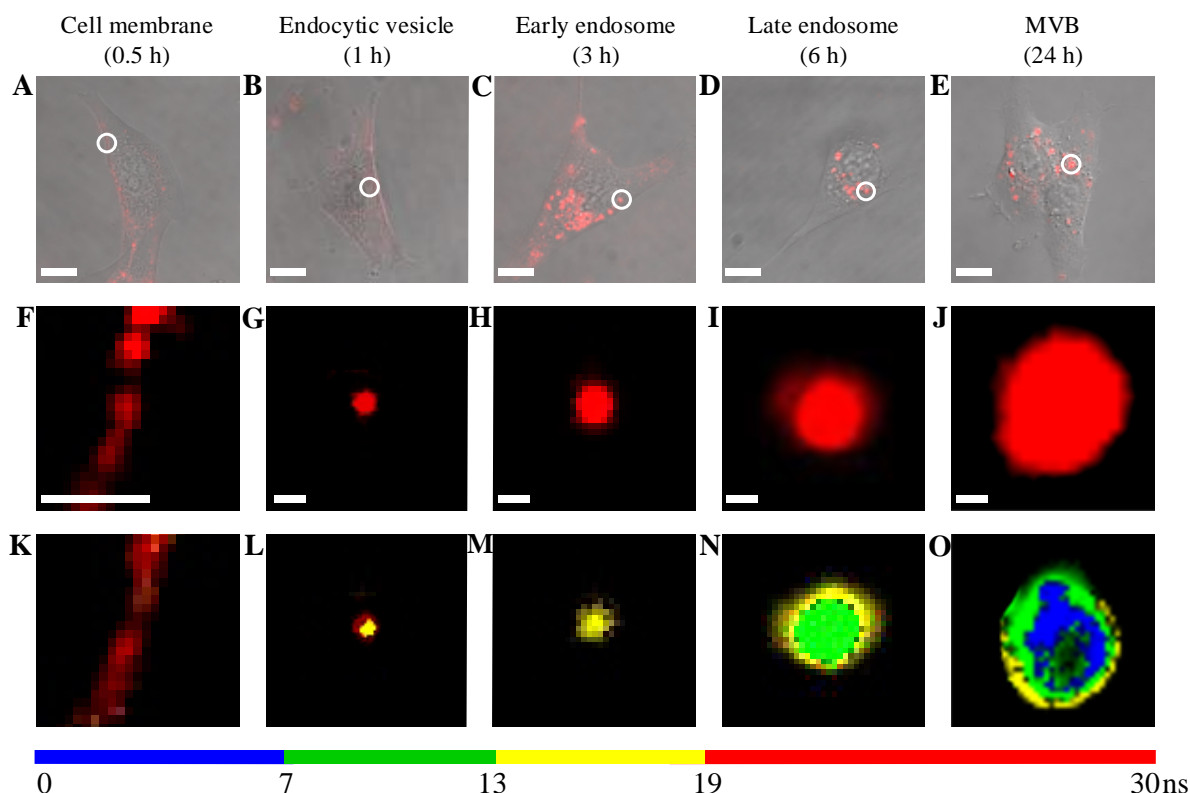


Figure 3: Overlaid phase contrast and confocal fluorescence images of NIH3T3 cells at different times of incubation with QDs revealing their intracellular distribution: A – QDs adherent to the membrane, B and C – endocytotic vesicles and early endosomes distributed in the cytoplasm, D – late endosomes are concentrated in a perinuclear region, E – multi-vesicular body-like structures distributed in the cytoplasm; scale bar: 10 μm . Confocal fluorescence images and fluorescence lifetime images of areas and vesicles marked with white circles in A-E: membrane (F, K), endocytotic vesicle (G, L), early endosome (H, M), late endosome (I, N) and MVB^[21] (J, O); scale bar: 1 μm . The lumen of early recycling endosomes has a pH value of 6.5–6.4 (as compared to pH 7.2 in the cytosol), that of late multivesicular endosomes has a pH of 6.0–5.0 and, after fusing with lysosomes, a pH of 5.0–4.5 is reached^[38]

At the first phase, when QDs adhere to the plasma membrane (Figure 3 A, F), the QDs mean PL lifetimes are the longest (Figure 3 K). When QDs are internalized into NIH3T3 cells, and the endocytic vesicles fully-filled with QDs are formed, the shorter mean PL lifetimes appear in the inner volume of the vesicle, which is still surrounded by the external structure exhibiting the longest PL lifetimes like those of QDs interacted with plasma membrane (Figure 3 B, G). An early endosome containing QDs had a quite homogenous structure (Figure 3 C, H), possessing only the shorter lifetimes. The vesicles bearing more complex structures appeared after the fusion of early endosomes with late endosomes. FLIM images revealed random distribution of different lifetimes in the outer area and even shorter lifetimes in the inner volume of the vesicles. The heterogeneous structure of multivesicular bodies was uncovered on the image when three time-gates were applied, and the shortest average lifetimes were detected in the central area (Figure 3 O, shown in blue). The green area seen in the middle most likely corresponds to a mixture of invaginated membranes and small intraluminous vesicles. The accumulation of internal membranes in vesicles starts at the stage of an early endosome and is thought to continue as it ‘matures’ to a late endosome.^[26] The lipid composition of late endosomes differs from that of earlier endocytic compartments, being enriched in triglycerides, cholesterol esters and selected phospholipids. Compared to the limiting membrane, the internal membranes of late endosomes/MVBs are heavily enriched in highly hydrophobic, cone shaped phospholipids dedicated to bend membranes for formation of MVBs.^[39]

One of important environmental factors affecting PL lifetime of intracellular QDs is the medium pH. By studying pH dependence of the PL of QDs in living cells it was found that cellular environment of low pH quenches QD photoluminescence,^[40] and that mean PL lifetimes being measured in membrane, cytoplasm or endosomes were shorter in more acidic pH.^[40] However, other studies noted that the lifetime of QDs in the acidic lysosomes (pH 4.5–5.0) was even shorter than that in a more acidic aqueous solution with a pH value of 2.20 thus demonstrating that the acidic environment is not the only cause for the shortening of the PL lifetimes of intracellular QDs. The photophysical properties of semiconductor QDs are sensitive to the processes taking place on their surface. The interaction between external biomolecules and those of QDs coating may enhance non-radiative decay and lead to the shortening of the mean PL lifetimes. The

analysis of PL decays of QDs in PBS (pH 7.4) containing different amino acids or proteins indicated that the higher concentration of amino acids resulted in a shorter PL lifetime.^[41] Moreover, the reduction of PL lifetimes was also observed for negatively charged QDs, which interact with positively charged intracellular proteins.^[42] One more assumption concerning the appearance of the shortest lifetimes detected at the last stage of QDs accumulation can be made on the grounds that QDs are more tightly packed in the mature endosomes and, therefore, can undergo a reduction in lifetime as a result of the energy transfer between QDs of different sizes in the ensemble of nanoparticles.^[42] Since the outer stabilizing layer (coating) of studied QDs is made of PEG with ionizable carboxylic acid groups, the interaction capacity of QDs also becomes pH-sensitive. Under low pH conditions the fraction of protonated COOH groups increases, which facilitates the formation of hydrogen bonds between the QDs coating and the biomolecules,^[41] also facilitating closer interaction between QDs.

It is clearly shown that the mean PL lifetimes of the intracellular carboxylated CdSe/ZnS QDs varied greatly depending on the intracellular localisation and related changes of intracellular microenvironment,^[43] which are related to both the QDs incubation time and their location within the cell. The changes in mean PL lifetimes of QD observed during their accumulation most likely are caused by the variations in biomolecular composition and acidity of the intracellular microenvironment altering molecular interactions of the QDs coating, which can affect the intrinsic photoluminescence characteristics of nanoparticles.

3.2 Uptake mechanism of quantum dots

3.2.1 Evaluation of QDs' passive diffusion through the cell membrane

The comparative study on the fate of QDs entering the cells via imitation of the passive diffusion has been performed, using the direct delivery approach. The strikingly contrasting distribution pattern of QDs photoluminescence was observed in cells after the intracellular microinjection (Figure 4, A, B in comparison with Figure 2). The injected QDs were instantly well dispersed across the entire cytoplasm. No formation of granular structures and no visible signs of aggregation were seen (Figure 4, A). The formation of QDs-containing vesicular structures was not observed afterwards as well (Figure 4, B). The observed time-dependent restructuring of QDs-containing vesicles

during the natural uptake and accumulation (changes in the size of the vesicles and formation of the multi-vesicular body-like structures) prompted us to investigate the intracellular migration of QDs, the possible fusion of QDs-containing vesicles and also the chances of QDs entrapped inside the vesicles to escape into the cytosol. EGFP transfected cells have been used to clarify those processes. The transfection itself had no influence on the phases of QDs accumulation in cells as well as on the formation and reshaping of red-luminescing endosomes (Figure 4, C). The dark and red-luminescing endosomes were detected on the background of the green fluorescence in EGFP transfected cells at 24 h after keeping them in a growth medium with QDs. The careful inspection of formed vesicles revealed small ($\sim 0.5 \mu\text{m}$) vesicles inside larger ($\sim 1.5 \mu\text{m}$) dark endosomes (Figure 4, D) implying the possible fusion of endosomes containing QDs with endosomes without QDs. However, no trace of the red PL of QDs dispersed across the entire cytosol was detected (Figure 4, C, D), as it was in case of the microinjection of QDs (Figure 4, A, B), and no appearance of yellow colour caused by the co-localization of red QDs with green EGFP was found. The presence or absence of protein in growth medium was found to have no influence on these observations.

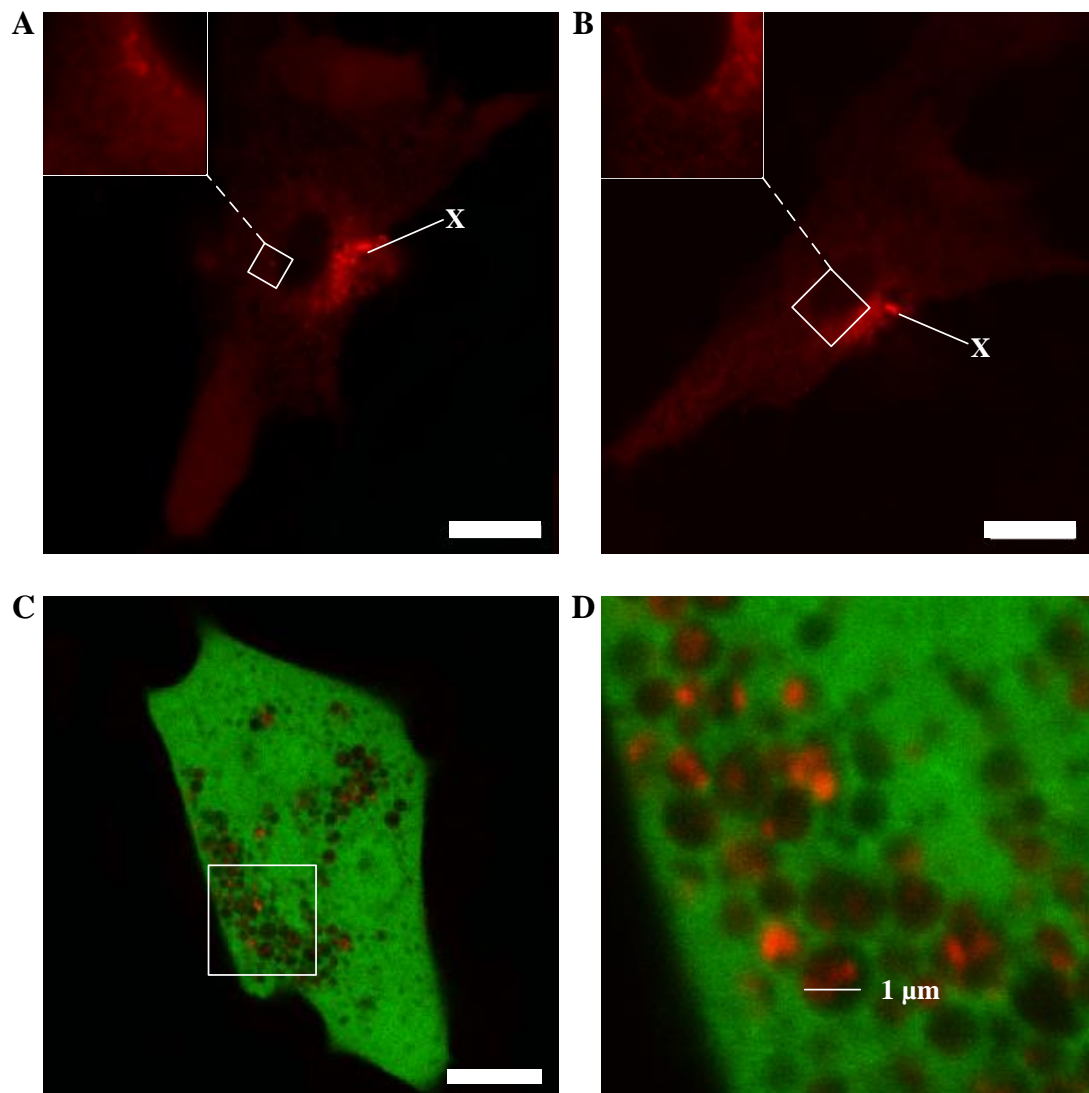


Figure 4: Confocal fluorescence images of NIH3T3 cells taken instantly after injection of QDs (A), 24 h after injection (B) and 24 h after incubation with QDs. X – injection site; white rectangles marks the zoomed parts which are shown in the inserts. Confocal fluorescence images of EGFP transfected NIH3T3 cells 24 h after incubation with QDs (C); D is zoomed part of B, showed with white rectangle.

Scale bar 10 μm

The direct delivery of QDs into cells is very limited in its throughput and is not suited for the manipulation of tens to hundreds of cells at a time, but is very valuable for achievement of the new research insights. This technique allows delivery of very small sample volumes (usually femtoliters) directly into the cytoplasm of individual cells avoiding the reaction with plasma membrane, which is the main barrier and the cause of intracellular vesicle formation during the natural uptake. In contrast to natural uptake, the microinjected QDs underwent no changes and remained uniformly distributed in

cytosol during the observation period (at least 24 h). Moreover, experiments with EGFP transfected cells confirmed the suggestion that QDs entrapped inside the vesicles during endocytosis could not escape to the cytosol. The vesicle fusion, which was evident in the phase 4 (Figure 2, D) and in the experiments on EGFP transfected cells (Figure 4, D) demonstrates that the natural uptake of QDs is impossible without endocytosis. Moreover, the transfer of QDs from endocytotic vesicles into cytosol or *vice versa* is restricted.

3.2.2 *Suppression of quantum dots' uptake*

To examine the role of saturation in the mechanism of QDs intracellular uptake, combined studies were conducted using primary and secondary QDs. The pretreatment of cells with primary QDs with PL peak at 545 nm (QD545) until the saturation phase (QD-saturated cells) resulted in a dramatically lower uptake rate of secondary QDs with PL peak at 625 nm (QD625) in cells. As shown in Figure 5, A, the accumulation of QD545 (used for the pretreatment of cells for 24 h) resulted in a granular distribution of green PL throughout the cytoplasm, while after 3 h of secondary treatment, QD625 were attached only to the cytoplasmic membrane of the pretreated cells. Moreover, no overlap of the red and green PL spots was observed, suggesting that the pretreatment with the primary QDs hindered the internalization of the secondary QDs in the cells. A different pattern was observed when secondary QDs were added to the medium of the pretreated cells at the growth stage. Evidence of co-localization of internalized primary QD545 (used for 1 h of pretreatment) and secondary QD625 was observed as yellow spots in confocal microscopy images in which the green and red channels were combined. These dots were distributed on the plasma membrane and in the cytoplasm (Figure 5, B).

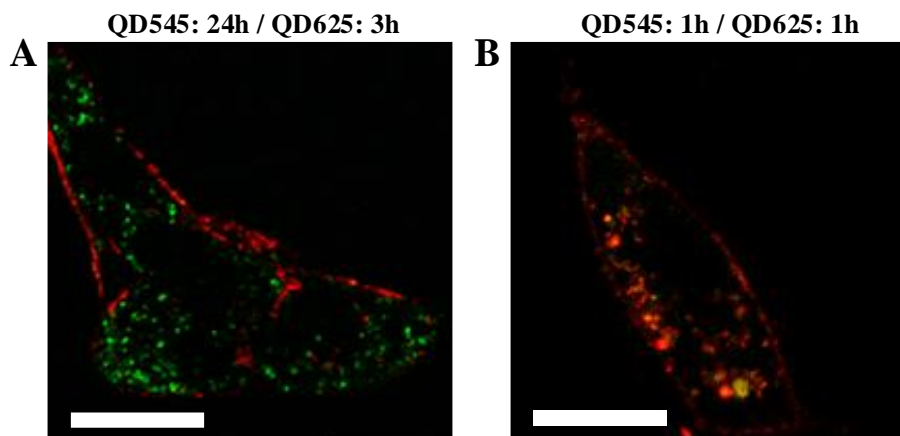


Figure 5: (A) A confocal fluorescence image obtained by combining the red and green channels to show the intracellular localization of quantum dots (QDs) with PL peak at 625 nm (QD625, red) after 3 h of incubation and QDs with PL peak at 545 nm (QD545, green), which was used for 24 h of pretreatment; (B) a confocal fluorescence image of NIH3T3 cells that were pretreated with QD545 for 1 h and then incubated with QD625 for 1 h. Scale bar = 20 μ m

The duration of pretreatment revealed the gradually reduced capacity of cells to accumulate secondary QDs with increasing times of pretreatment with primary QDs: a strong reduction in the PL intensity of secondary QDs was reported even after 3 or 6 h of pretreatment, and the internalization capacity of the pretreated cells was almost totally suppressed after 24 h. Confocal microscopy imaging revealed that under such conditions, secondary QD625 was present on the plasma membrane of the pretreated cells (Figure 5, A); however, adherence to the plasma membrane was not sufficient for the uptake of QD625, as no secondary QDs were detected inside the cells, even after 3 h of incubation.

3.2.3 Reinitiation of quantum dots' uptake

The pretreated cells were further studied to determine the duration of the suppression stage of QD uptake until its expected reinitiation. This time, after 24 h of pretreatment with QD625, the relative PL intensities of the accumulated QDs, which were normalized per cell, were monitored in two experiments (Figure 6, A). First, the PL intensity of the QDs continually diminished in cells that were rinsed and subsequently incubated in medium without QDs (Figure 6, A, empty squares). This reduction in intensity per cell can be explained by cell division, as the total PL intensity calculated per cell of the QDs present in divided cells does not change (Figure 6, B). In the second case, the pretreated cells were first incubated in medium without QDs for different time intervals and then a

new dose of QD625 (arrows in Figure 6, A) was added to the medium for an additional 1 h of incubation prior to the measurements. The mean intensities of the overall PL from the accumulated QDs, which were measured at 24+3 h and 24+6 h (Figure 6, A, black squares), followed the same tendency as that observed for the cells incubated in medium without QDs (Figure 6, A, empty squares), indicating that the uptake of the QDs was still not restored. However, as detected after 24+8 h, the mean PL per cell almost reached the initial level of intensity that is typical for saturation in cells incubated with QDs for 24 h.

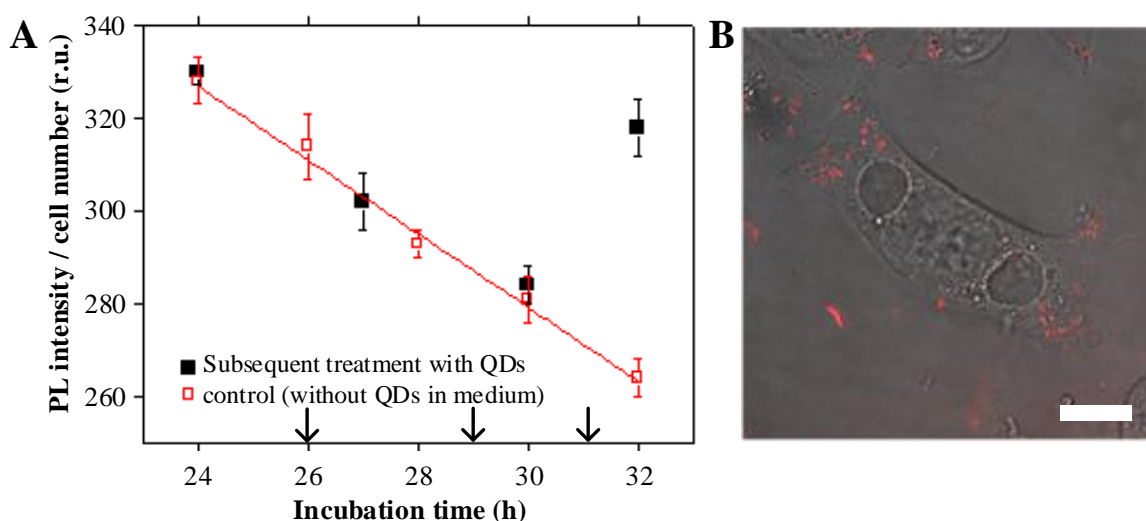


Figure 6: (A) Reinitiation of QD uptake. The arrows mark the times of QD addition into the medium. (B) Overlay of phase contrast and fluorescence images of a dividing cell with internalized QD625 after 24 h of incubation. Scale bar = 10 μ m

The imaging of the cells by means of the phase contrast and confocal fluorescence microscopy demonstrated that when the cells were dividing, the internalized QDs were redistributed among the daughter cells, reducing the total amount of QDs per cell (Figure 6, B). Some studies, in which the dependence of internalization of nanoparticles on the cell cycle phase was investigated, also showed that cell division dilutes the intracellular concentration of nanoparticles.^[44] The addition of QDs into the incubation medium of pretreated cells at 2 or 5 h had no effect on the subsequently (1 h later) measured mean PL intensities (Figure 6, A, black squares). However, the PL signal that was measured 1 h after the addition of QDs at 7 h revealed restored PL intensity values, implying the reinitiation of QD uptake by the cells. The observed delay in this reinitiation may be related to the natural replenishment of substances that participate in endocytosis in newly

divided cells. This apparent capacity of cells to suppress and resume the uptake of non-targeted QDs supports the idea that the uptake occurs via single endocytotic mechanism.

3.2.4 *Uptake mechanism of quantum dots*

Transferrin (Trf) was selected to examine the suppressive effect induced by carboxyl-coated QDs on the uptake mediated by clathrin-dependent endocytosis. The mean values of the Trf fluorescence intensities, which were measured spectroscopically at various times of simultaneous incubation with QDs in control cells (empty squares) and in QD-saturated cells (full squares) were the same within the margin of error Figure 7, A. The confocal fluorescence microscopy image of Trf in the control cells (green channel, Figure 7, B) illustrates that after 1 h of incubation Trf was localized on the plasma membrane and also formed a granular pattern in the cytoplasm. The images of the cells, which were incubated with QDs (seen in red vesicles in the cytoplasm) for 24 h until the saturation stage and then incubated for 1 h with Trf, demonstrated the similar intracellular distribution of Trf. (Figure 7, C). Some of the observed vesicles were yellow in colour, implying the co-localization of Trf within the vesicles containing QDs.

An insignificant suppressive effect of accumulated QD625 was also observed on the uptake of dextran (DexB), a marker of macropinocytosis^[46] (Figure 7, D-F). Comparable mean intensity values for blue fluorescence of DexB were detected in all of the cell suspensions independent of the pretreatment of the cells with QDs for almost all of the examined incubation times (Figure 7, D).

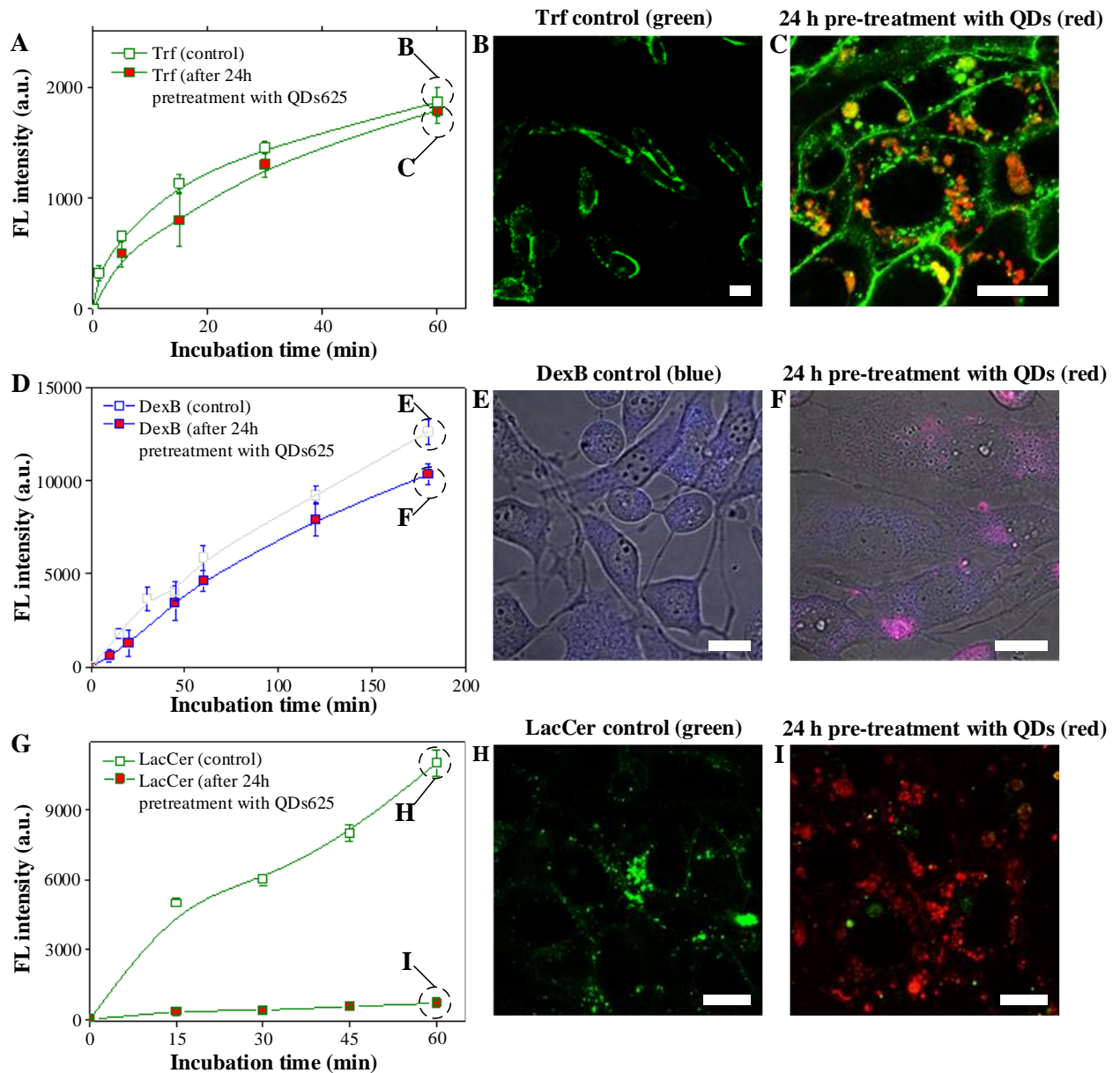


Figure 7: Effect of incubation of NIH3T3 cells with QD625 until the saturation stage on the clathrin-dependent (A-C), macropinocytosis (D-F) and lipid raft/caveolin-dependent (G-I) pathways of endocytosis. (A) Dynamics of the intracellular uptake of Trf by untreated (control) cells and cells that were incubated with QD625 for 24 h, assessed by fluorescence spectrometry. Confocal fluorescence microscopy images of the intracellular localization of Trf (green) after 1 h in control cells (B) and cells that were incubated with QD625 (C, red). Scale bar = 20 μ m. (D) Dynamics of the intracellular uptake of DexB by control cells and cells that were incubated with QD625 for 24 h, assessed by PL spectrometry. Overlaid fluorescence microscopy and phase contrast images of the intracellular localization of DexB (blue) at 3 h in control cells (E) and cells that were incubated with QD625 for 24 h (F, pink). (G) Dynamics of the intracellular uptake of LacCer by untreated (control) NIH3T3 cells and cells that were incubated with QD625 for 24 h, assessed by PL spectrometry. Confocal fluorescence microscopy images of the intracellular localization of LacCer (green) after 1 h in control cells (H) and cells that were incubated with QD625 (I, red). Scale bar = 10 μ m

In contrast, the uptake of lactosylceramide (LacCer), a well-known caveolae ligand that is selectively internalized via caveolae in mammalian cells,^[47] was almost completely prevented in QD-saturated cells, resulting in obvious differences in the PL spectroscopy data (Figure 7, G-I). The suppression of LacCer uptake was further confirmed by comparing the confocal microscopy images of control and treated cells after 1 h of incubation (Figure 7, H and I, respectively). The LacCer fluorescence pattern (green channel) in the control cells was very similar to the typical intracellular PL pattern of QDs. At the same time, only scarce green-fluorescing spots were observed among the prevailing red fluorescence in the treated cells.

Deeper insight into the QD uptake mechanism was gained by transiently transfecting NIH3T3 cells with the plasmid EGFP-C1-Caveolin-1 to visualize the intracellular distribution of caveolin-1 (member of caveolin gene family), a scaffolding molecule that is essential for driving membrane curvature and the formation of caveolae structures.^[48,49] The impact of incubation with QD625 for 3 h or 24 h on the distribution of caveolin-1 is shown in Figure 8.

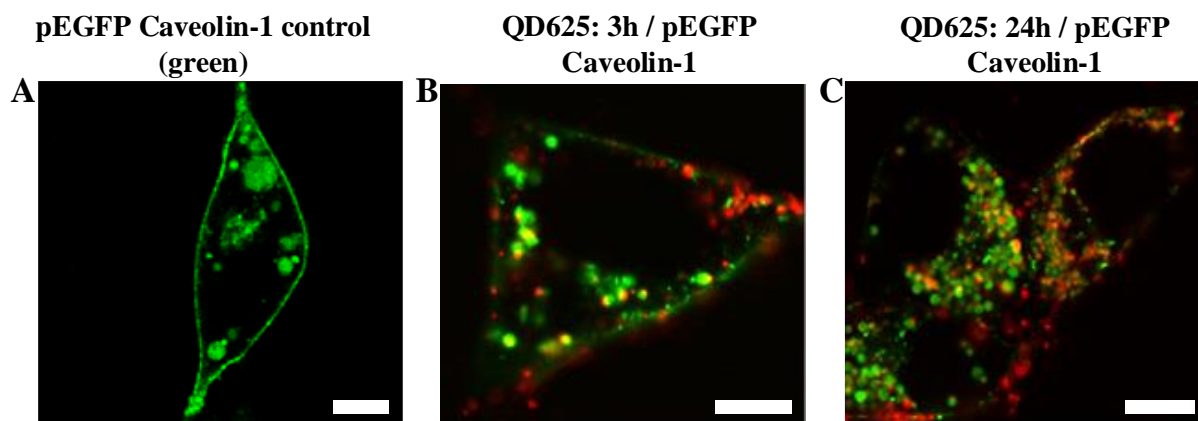


Figure 8: Confocal fluorescence images of the intracellular distribution of Caveolin-1 (green) in control cells (A) and cells that were treated with QD625 (red) for 3 h (B) or 24 h (C). Scale bar = 10 μm

The expression of pEGFP-Caveolin-1 yielded differently sized (0.5-3.5 μm in diameter) green-fluorescing vesicular structures in the cytoplasm and even in the plasma membrane (Figure 8, A). The co-localization of QDs and EGFP-Caveolin-1 after 3 h of incubation was observed as yellow spots in confocal microscopy images, in which the green and the red channels were combined. These spots were distributed on the plasma

membrane and in the cytoplasm (Figure 8, B). The number of vesicles ($\sim 1 \mu\text{m}$ in diameter) considerably increased, and the green staining of the cell membrane was no longer observed when the QD accumulation reached the saturation stage (Figure 8, C).

3.3 Overview of the process and mechanism of quantum dots' intracellular uptake

To summarize the presented results and discussed references, a scheme is suggested to illustrate both the potential mechanism for the intracellular uptake of non-targeted, negatively charged quantum dots via caveolin-mediated endocytosis and its suppression (Figure 9).

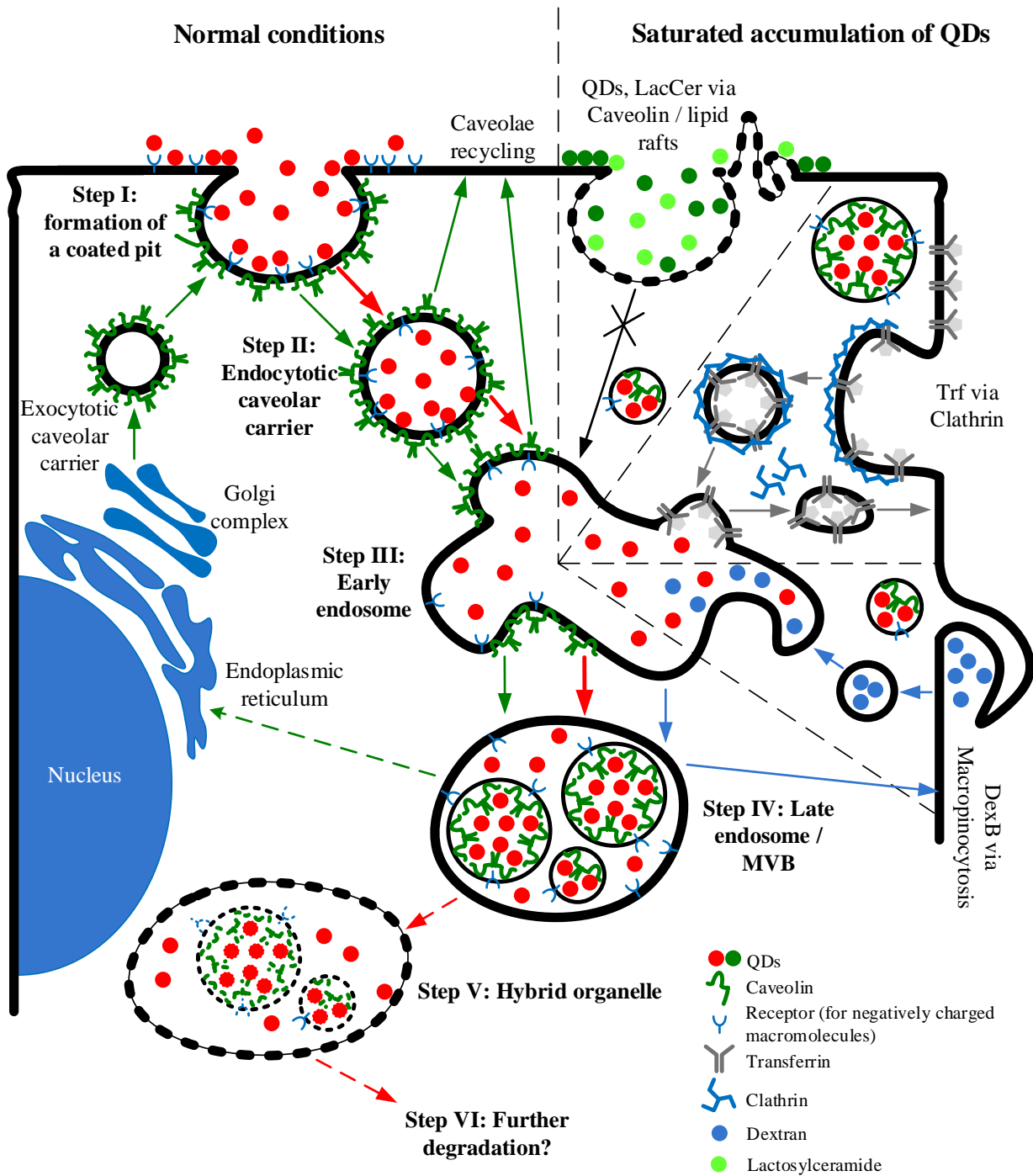


Figure 9: Scheme of the intracellular uptake of QDs via caveolin-dependent endocytosis and the influence of a saturating accumulation of QDs (red arrows). The membrane trafficking of caveolin via exocytosis and endocytosis under normal conditions is based on the findings of R.G. Parton et al.^[49] (green arrows), and the hybrid organelle was previously described by J.P. Luzio et al.^[50] and A. Hayer et al.^[51] The pathway for Trf via clathrin-dependent endocytosis is marked with grey arrows, and that for DexB via macropinocytosis is marked with blue arrows. The still unclear routes are marked with dashed lines.

During internalization into early endosomes (Steps I to III), receptors can be sorted for recycling and then travel back to the cell surface. The overall rate of endocytic internalization of the plasma membrane is quite high; cultured fibroblasts regularly internalize 50% of their cell surface proteins and phospholipids each hour. Most cell surface receptors that undergo endocytosis repeatedly deposit their ligands within the cell and then return them to the plasma membrane to, once again, mediate the internalization of ligand molecules. For instance, the low-density lipoprotein (LDL) receptor makes one round trip into and out of the cell every 10 to 20 minutes, for a total of several hundred trips in its 20-hour life span before the receptor–ligand complex is degraded in lysosomes, reducing the number of cell surface receptors.^[52] Some endocytosed ligands dissociate from their receptors in the acidic lumen of early endosomes and are delivered to lysosomes for degradation. This process also allows for the subsequent recycling of the empty receptors to the cell surface. Other ligands remain bound to their receptors (which are ubiquitinated), and after endocytosis, the receptor–ligand complexes are internalized from the endosomal surface into luminal vesicles. Late endosomes (LEs) containing these luminal vesicles fuse with lysosomes.^[50] The latter pathway (Step IV) is intended for the receptors associated with caveolae, which are directed into the intraluminal vesicles of multivesicular bodies, resulting in slower receptor turnover and signal termination.^[53] Because the disassembly of the highly stable, long-lived caveolae and the degradation of caveolin can only occur in late endosomes/lysosomes (LE/LYSs)^[51] or hybrid organelles^[50] and because MVBs containing QDs are still observed after 96 h, the saturation and suppression effects of caveolin-mediated endocytosis can be induced. Accordingly, the reinitiation of QD internalization detected after ~8 h (Figure 6, A) could be the result of the restored turnover of the receptor and caveolin, which presumably involves biosynthetic processes that are initiated after cell division. Then, the newly divided cells are able to proceed with the internalization of QDs as long as nanoparticles are present in the medium. Caveolin-1 is an integral membrane protein.^[54] Detailed morphological and biochemical studies of fibroblasts^[55] have shown that under normal conditions, caveolin-1 in caveolae-derived vesicles constitutively cycles between the cell membrane and Golgi apparatus (where it is incorporated into lipid domains that sort molecules for shipment to the cell surface), spending part of its time as a luminal protein of the endoplasmic

reticulum. The preferred location of caveolin at the cell surface is the caveola.^[54] Caveolae are long-lived, plasma membrane microdomains that are composed of caveolins, cavins and a cholesterol-rich membrane. Studies on caveolae disassembly and the degradation of their coat components have shown that caveolin-1 is degraded very slowly, but turnover can be accelerated by compromising caveolae assembly. Normally, caveolae-derived vesicles follow the endocytic trafficking route to lysosomes.^[51] The formed caveolae fuse with early endosomes, where efficient sorting occurs. Caveolin-1 can be trafficked into and from early endosomes. Recycling endosomes mediate caveolin trafficking back to the surface. Upon early endosomal maturation, caveolin-1 is detected in the intraluminal vesicles of LEs and found to be degraded in modified LE/LYSs.

However, our results showed that in the case of QD uptake, when QDs are internalized through the caveolin-dependent pathway, the normal cycling of caveolin-1 is interrupted due to some interaction between the QDs and caveolin-1 and its relocation from the cell membrane to the vesicles. Two possible options can be considered here. Such an interaction could lead to an irreversible interruption, meaning that the trapped caveolin-1 is not recycled to the surface of the membrane through the common cycling route. The reinitiation of uptake becomes possible only due to the synthesis of new caveolin. Alternatively, it is recycled, albeit very slowly. Presumably, caveolin-1 may be recycled and trafficked to the endoplasmic reticulum (via Step V) or degraded (via Step VI), although the routes mediating such recycling and degradation remain unclear (dashed lines in Figure 9).

3.4 Precautions for the combined application of QDs and biomedical agents

The observed discriminating suppressive effect of carboxyl-coated QDs on the uptake of certain agents prompted us to examine the possibility of combining these nanoparticles with certain anticancer agents, as such a combination would allow for diagnostic visualization and potential theranostic effects. *in vitro* experiments revealed that pretreatment of NIH3T3 cells with QD545 did not suppress the uptake of the photosensitizer chlorin e6 (Ce_6) (Figure 10, A), which is commonly used in photodynamic therapy.^[56] Ce_6 is an amphiphilic molecule that binds to the plasma membrane and either passively penetrates through it^[57] or is taken up by bulk endocytosis and is trafficked through the endocytosis pathway mediated by the LDL

receptor.^[58] A diffuse distribution of red Ce₆ fluorescence was detected in the confocal fluorescence microscopy images of QD-saturated cells (Figure 10, A), together with green intravesicular photoluminescence from the QDs. There were no yellow spots (indicating the co-localization of Ce₆ fluorescence and QD photoluminescence) after 2 h of incubation with Ce₆. On the other hand, the same incubation with QD545 had an impact on the chemotoxicity of cisplatin, a widely used anticancer drug^[59] that crosses the plasma membrane through several specific transporters.^[60] The experiments of treatment with cisplatin showed that QD-saturated cells had a higher resistance (Figure 10, B). The viability of the cells treated with 0.5 µg/mL of cisplatin increased from 50% in control cells to almost 80% in QD-saturated cells. No cytotoxic effects of QDs alone were observed on cell viability or proliferation at the tested concentrations during the experimental incubation times.

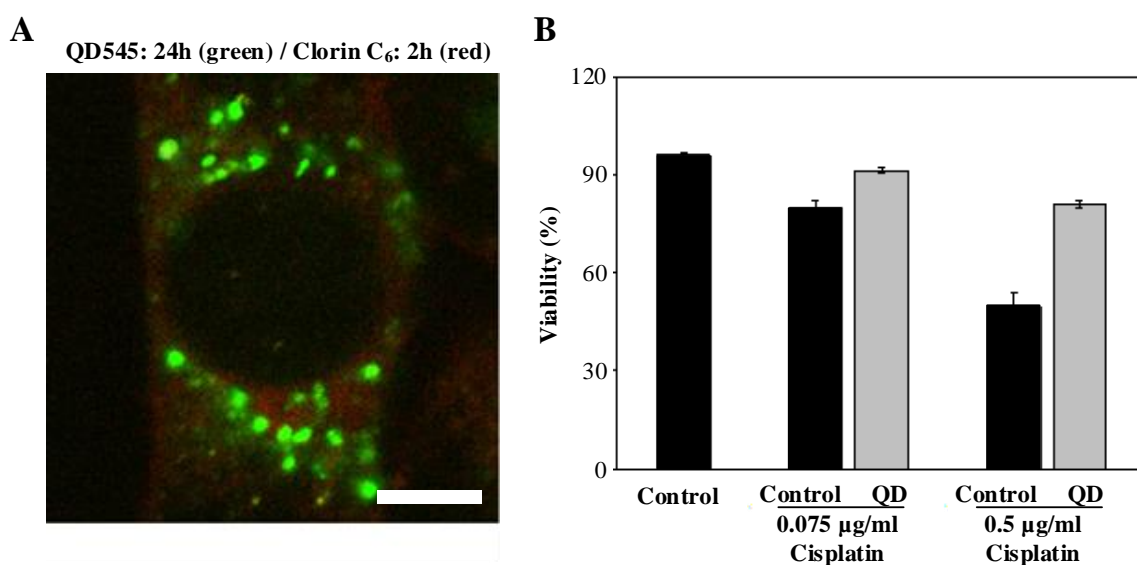


Figure 10: Fluorescence confocal microscopy image of the intracellular localization of Ce₆ (red) after 2 h of incubation in cells that were incubated with QD545 (green) for 24 h (A). Scale bar = 10 µm. (B) Increased resistance of NIH3T3 cells to cisplatin, induced by incubation with QD545 for 24 h

A lower chemotoxic effect in the QD-saturated cells than in the control cells could have been caused, for instance, by the reduced accumulation of cisplatin – if the internalization of this particular drug was also suppressed by incubation with QDs. However, the cellular internalization channel used for uptake of nanoparticles depends on the surface charge and is selective for either positively or negatively charged QDs.^[61]

^{63]} Because cisplatin is positively charged at physiological pH (pKa = 6.56)^[64] and is internalized by cells through copper and cation transporters,^[60] it seems that negatively charged QDs shouldn't have any influence on these receptors to suppress the uptake of cisplatin. Moreover, these QDs also did not influence the uptake of the amphiphilic photosensitizer chlorin e6. Thus, one can assume that a saturating accumulation of negatively charged QDs directly affects only SRA and the receptors involved in caveolin/lipid raft-related endocytosis, which is characteristic of negatively charged molecules.^[63,65] Therefore, it is more likely that QD internalization affects cisplatin via a different mechanism, presumably inducing stress responses rather than releasing its core metal ions.^[66]

It has been shown that carboxyl-coated PEG-QDs trigger the activation of NF-κB and MAPK signalling (two major signalling cascades that participate in pro-inflammatory responses) as well as the production of cytokines/chemokines in human skin cells and primary monocytes, respectively.^[63] There are also publications showing that the NF-κB activation in fibroblasts drives the autophagic degradation of Caveolin-1^[67] suggesting that oxidative stress-induced autophagy is a defence/survival mechanism against the cytotoxicity of QDs.^[68] Moreover, some studies have indicated that the cells experiencing deficiency in Caveolin-1, become more resistant to oxidative stress-induced cytotoxicity.^[69] Therefore, we assume that saturating accumulation of carboxylated QDs, which were found to be internalized via the caveolin-mediated endocytotic pathway, might induce Caveolin-1 deficiency related stress signals, such as the triggering of autophagy, which consequently led to an increased resistance to cisplatin.^[67,70]

Non-targeted, carboxylated QDs bearing a negative charge are suitable tools for modeling studies of non-specific nanoparticle uptake and intracellular trafficking.^[71] Most studies to date have suggested that the generation of reactive oxygen species (ROS), which can be either protective or harmful during biological interactions,^[72] and the resultant oxidative stress are frequently induced by many types of nanoparticles, which vary in size, surface reactivity and dose-dependent toxicity,^[73,74] thus indicating ROS as a key route of nanoparticle cytotoxicity.^[75] Nanoparticle-induced oxidative stress responses are followed by the activation of associated stress-dependent cellular signalling pathways and the occurrence of various pathophysiological effects, including

genotoxicity, inflammation, apoptosis, lipid peroxidation and fibrosis.^[72] The possible relationship between the long-term accumulation of nanoparticles and the induced cellular stress should be particularly considered for nanoparticles intended for cancer therapy, including gold,^[76] polystyrene,^[77] polymeric,^[65] mesoporous silica^[78] and iron oxide^[79] nanoparticles, paying attention to their properties, such as size, pegylation, surface functionality, targeting ligands, charge and shape, which direct nanoparticles to internalization through caveolin/lipid raft-mediated pathways. The complexity of the outcomes for combined therapy is illustrated not only by our findings of the induced cell resistance to cisplatin due to a saturating accumulation of QDs, but also by other studies showing that the Caveolin-1 deficiency and autophagy triggered by oxidative stress in cancer-associated fibroblasts fuels tumour growth, while autophagy in cancer cells retards tumour growth.^[67] It is, therefore, very important to functionalize the surface of nanoparticles in such a way that would allow for the control or the prevention of oxidative stress induction.^[80]

Moreover, *in vivo*, all nanoparticles reach their target site (e.g., tumour) via passive selectivity, and the attachment of affinity ligands to the particles does not increase the amount that reaches the target but rather promotes the final step of intracellular uptake.^[81] Targeting efficiency is related to the density of the receptors on the cell surface.^[82] Therefore, in most cases, non-specific binding and uptake occurs due to the insufficient affinity of the ligand, hindered internalization, low antigen density and/or 'binding site' barriers.^[81] Reducing both the non-specific binding of nanoparticles to biomolecules and the uptake of nanoparticles by the reticuloendothelial system is a major challenge for improving the sensitivity and specificity of biomarker-targeted nanoparticles *in vivo*.^[83] However, non-specific internalization is required for a substance to be internalized as efficiently as possible^[31] and reduced adhesion to the cell membrane results in decreased uptake by the targeted cells.^[84] The effective uptake of nanoparticle could be achieved by combining several strategies. For example, the potential to maximize the specific uptake into the targeted cells while minimizing non-specific uptake lies in the formation of a double-charged, zwitterionic surface coating for nanoparticles,^[83] containing a negatively charged -PEG-carboxyl group and an optimal density of positively charged, PEG-targeting ligands.

4 Conclusions

1. The investigation of intracellular uptake of non-targeted negatively charged quantum dots with fluorescence spectroscopy method revealed three time-related accumulation stages: I – a plateau stage, II – a growth stage and III – a saturation stage, which are characteristic for all investigated cell lines, but the stages were of different timing for each of the investigated cell line.
2. The confocal fluorescence microscopy imaging showed the intracellular localisation phases of accumulated QDs based on type and localisation of formed vesicles: 1 – adherence to the cell membrane; 2 – formation of granulated clusters spread in the cytoplasm; 3 – localization of granulated clusters in a perinuclear region; and phase 4 – formation of multi-vesicular bodies and their redistribution in the cytoplasm.
3. The fluorescence lifetime imaging microscopy revealed the inner heterogeneity of intracellular vesicles: the endosomes at particular stage of maturity can be identified by different photoluminescence lifetimes of accumulated QDs: 16-22 ns for endocytic vesicles, 10-15 ns for early endosomes and 5-9 ns for late endosomes and multivesicular bodies.
4. Quantum dots do not penetrate the plasma membranes of cells through passive diffusion, but enter a cell through endocytosis. Negatively charged quantum dots without protein corona enter the cells through the single, caveolin-dependent endocytic pathway.
5. Examination of the possibility to combine quantum dots, as model diagnostic probes, with anticancer agent cisplatin *in vitro* revealed, that despite QDs alone had no cytotoxic effects on cells viability and proliferation, they increased drug resistance. Therefore, this effect needs profound further research before the application of quantum dots in combined diagnosis and therapy *in vivo*.

5 References

1. C. Vauthier, P. Couvreur, E. Fattal. Nanomaterials: Applications in Drug Delivery. p. 131-151. Nanomaterials: A danger or a promise? A chemical and biological perspective. Redaktoriai: R. Brayner, F. Fiévet, T. Coradin. Springer, 2013 (elektroninè knyga)
2. L.Y. Rizzo, B. Theek, G. Storm, F. Kiessling, T. Lammers. Recent progress in nanomedicine: therapeutic, diagnostic and theranostic applications. *Current Opinion in Biotechnology*. 24, 6: 1159–1166 (2013)
3. L. Brannon-Peppas, J.O. Blanchette. Nanoparticle and targeted systems for cancer therapy. *Advanced Drug Delivery Reviews*. 64: 206–212 (2012)
4. A.Z. Wang, R. Langer, O.C. Farokhzad. Nanoparticle delivery of cancer drugs. *Annu. Rev. Med.* 63: 185–98 (2012)
5. J. Panyama, V. Labhasetwar. Biodegradable nanoparticles for drug and gene delivery to cells and tissue. *Advanced Drug Delivery Reviews*. 64: 61–71 (2012)
6. J. Breger, J.B. Delehanty, I.L. Medintz. Continuing progress toward controlled intracellular delivery of semiconductor quantum dots. *Nanomedicine and Nanobiotechnology*. 6, 5 (2014)
7. M.J.D. Clift, V. Stone. Quantum dots: an insight and perspective of their biological interaction and how this relates to their relevance for clinical use. *Theranostics*. 2, 7: 668–680 (2012)
8. F.M. Winnik, D. Maysinger. Quantum dot cytotoxicity and ways to reduce it. *Acc Chem Res*. 19, 46(3): 672–680 (2013)
9. C.E. Probst, P. Zrazhevskiy, V. Bagalkot, X. Gao. Quantum dots as a platform for nanoparticle drug delivery vehicle design. *Advanced Drug Delivery Reviews*. 65: 703–718 (2013)
10. S. Ghaderi, B. Ramesh, A. M. Seifalian. Fluorescence nanoparticles “quantum dots” as drug delivery system and their toxicity: a review. *Journal of Drug Targeting*. 19, 7: 475–486 (2011)
11. F. Joris, B.B. Manshian, K. Peynshaert, S.C. Smedt, K. Braeckmans, S.J. Soenen. Assessing nanoparticle toxicity in cell-based assays: influence of cell culture parameters and optimized models for bridging the *in vitro*–*in vivo* gap. *Chem. Soc. Rev.* 42: 8339–8359 (2013)
12. A. Albanese, P.S. Tang, W.C. Chan. The effect of nanoparticle size, shape, and surface chemistry on biological systems. *Annu Rev Biomed Eng*. 14: 1–16 (2012)
13. A. E. Nel, L. Mädler, D. Velegol, T. Xia, E.M.V. Hoek, P. Somasundaran, F. Klaessig, V. Castranova, M. Thompson. Understanding biophysicochemical interactions at the nano–biointerface. *Nature Materials*. 8, 7: 543–557 (2009)
14. R. Duncan, R. Gaspar. Nanomedicine(s) under the microscope. *Mol. Pharmaceutics*. 8: 2101–2141 (2011)
15. M. Zhu, G. Nie, H. Meng, T. Xia, A. Nel, Y. Zhao. Physicochemical properties determine nanomaterial cellular uptake, transport and fate. *Acc. Chem. Res.* 46, 3: 622–631 (2013)
16. L.O. Cinteza. Quantum dots in biomedical applications: advances and challenges. *J. Nanophoton.* 4, 1: 042503 (2010)

17. B. Wang, X. He, Z. Zhang, Y. Zhao, W. Feng. Metabolism of nanomaterials in vivo: blood circulation and organ clearance. *Acc. Chem. Res.* 46, 3: 761–769 (2013)
18. N.M. Zaki, N. Tirelli. Gateways for the intracellular access of nanocarriers: a review of receptor-mediated endocytosis mechanisms and of strategies in receptor targeting. *Expert Opin Drug Deliv.* 7, 8: 895–913 (2010)
19. T.G. Iversen, T. Skotland, K. Sandvig. Endocytosis and intracellular transport of nanoparticles: present knowledge and need for future studies. *Nano Today.* 6: 176–185 (2011)
20. V.A. Torres, J.C. Tapia, D.A. Rodriguez, M. Parraga, P. Lisboa, M. Montoya, L. Leyton, A.F. Quest, Caveolin-1 controls cell proliferation and cell death by suppressing expression of the inhibitor of apoptosis protein survivin. *J. Cell Sci.* 119: 1812–1832 (2006)
21. V. Karabanovas, Z. Zitkus, D. Kuciauskas, R. Rotomskis and M. Valius. Surface properties of quantum dots define their cellular endocytic routes, mitogenic stimulation and suppression of cell migration. *J. Biomed. Nanotechnol.* 10: 775–786 (2014)
22. B.D. Grant, J.G. Donaldson. Pathways and mechanisms of endocytic recycling. *Nat Rev Mol Cell Biol.* 10(9): 597-608 (2009)
23. I. Dikic. Endosomes Molecular Biology Intelligence Unit. New York: Landes Bioscience, Springer Science+Business Media, LLC, 2006 (elektroninė knyga)
24. M. Pavelka, J. Roth. Functional Ultrastructure: An Atlas of Tissue Biology and Pathology. 2nd ed. Wien: SpringerWienNewYork, 2010 (elektroninė knyga)
25. K. Abe, H. Takano, T. Ito. Appearance of peculiar multivesicular bodies in the principal cells of the epididymal duct after efferent duct cutting in the mouse. *Arch Histol Jpn.* 47, 2: 121–135 (1984)
26. A. Sorkin, M. von Zastrow. Endocytosis and signalling: intertwining molecular networks. *Nat Rev Mol Cell Biol.* 10, 9: 609–622 (2009)
27. K.L. Douglas, C.A. Piccirillo, M. Tabrizian. Cell line-dependent internalization pathways and intracellular trafficking determine transfection efficiency of nanoparticle vectors. *Eur J Pharm Biopharm.* 68: 676–687 (2008)
28. A. Hoshino, K. Hanaki, K. Suzuki, K. Yamamoto. Applications of T-lymphoma labeled with fluorescent quantum dots to cell tracing markers in mouse body. *Biochem Biophys Res Commun.* 30, 314(1): 46–53 (2004)
29. M.J. Clift, C. Brandenberger, B. Rothen-Rutishauser, D.M. Brown, V. Stone. The uptake and intracellular fate of a series of different surface coated quantum dots in vitro. *Toxicology.* 15, 286(1-3): 58–68 (2011)
30. W. Jiang, B.Y.S. Kim, J.T. Rutka, W.C.W. Chan. Nanoparticle-mediated cellular response is size-dependent. *Nature Nanotechnology* 3, 145–150 (2008)
31. T.A. Kelf, V.K. Sreenivasan, J. Sun, E.J. Kim, E.M. Goldys, A.V. Zvyagin. Non-specific cellular uptake of surface-functionalized quantum dots. *Nanotechnology.* 16, 21(28): 285105 (2010)

32. Y. Williams, A. Sukhanova, M. Nowostawska, A. M. Davies, S. Mitchell, V. Oleinikov, Y. Gun'ko, I. Nabiev, D. Kelleher, Y. Volkov. Probing cell-type-specific intracellular nanoscale barriers using size-tuned quantum dots. *Small*. 5, 22: 2581–2588 (2009)
33. F. Corsi F, C. Palma, M. Colombo. Towards ideal magnetofluorescent nanoparticles for bimodal detection of breast-cancer cells. *Small*. 5: 2555–2564 (2009)
34. L.W. Zhang, N.A. Monteiro-Riviere. Mechanisms of quantum dot nanoparticle cellular uptake. *Toxicol Sci*. 110, 1: 138–155 (2009)
35. Y. Xiao, S.P. Forry, X. Gao, R.D. Holbrook, W.G. Telford, A. Tona. Dynamics and mechanisms of quantum dot nanoparticle cellular uptake. *J Nanobiotechnology*. 15, 8: 13 (2010)
36. W.J. Parak, T. Pellegrino, C. Plank. Labelling of cells with quantum dots. *Nanotechnology*. 16: 9–25 (2005)
37. Y. Yuan, C. Liu, J. Qian, J. Wang, Y. Zhang. Size-mediated cytotoxicity and apoptosis of hydroxyapatite nanoparticles in human hepatoma HepG2 cells. *Biomaterials*. 31: 730–740 (2010)
38. R. Dobrowolski and E.M. De Robertis. Endocytic control of growth factor signalling: multivesicular bodies as signalling organelles. *Nat Rev Mol Cell Biol*. 13, 1: 53–60 (2012)
39. R.C. Piper and J.P. Luzio. Late endosomes: sorting and partitioning in multivesicular bodies. *Traffic*. 2, 9: 612–621 (2001)
40. Y.S. Liu, Y.H. Sun, P.T. Vernier, C.H. Liang, S.Y.C. Chong and M.A. Gundersen. pH-sensitive photoluminescence of CdSe/ZnSe/ZnS quantum dots in human ovarian cancer cells. *J. Phys. Chem. C*. 111: 2872–2878 (2007)
41. J. Conroy, S.J. Byrne, Y.K. Gunko, Y.P. Rakovich, J.F. Donegan, A. Davies, D. Kelleher, Y. Volkov. CdTe nanoparticles display tropism to core histones and histone-rich cell organelles. *Small*. 4, 11: 2006–2015 (2008)
42. Y. Zhang, L. Mi, J. Chen, P. Wang. The environmental influence on the photoluminescence behavior of thiol-capped CdTe quantum dots in living cells. *Biomed. Mater*. 4: 012001 (2009)
43. J.R. Lakowicz, H. Szmajcinski, K. Nowaczyk, K. W. Berndt and M. Johnson. Fluorescence lifetime imaging. *Anal. Biochem*. 202: 316–230 (1992)
44. J.A. Kim, C. Aberg C, A. Salvati, K.A. Dawson. Role of cell cycle on the cellular uptake and dilution of nanoparticles in a cell population. *Nat. Nanotechnol*. 7: 62–68 (2012)
45. C.L. Roy, J.L. Wrana. Clathrin- and non-clathrin mediated endocytic regulation of cell signaling. *Nature Reviews Molecular Cell Biology*. 6: 112–126 (2005)
46. M.K. Zenni, P.C. Giardina, H.A. Harvey, J. Shao, M.R. Ketterer, D.M. Lubaroff, R.D. Williams, M.A. Apicella. Macropinocytosis as a mechanism of entry into primary human urethral epithelial cells by neisseria gonorrhoeae. *Infect Immun*. 68, 3: 1696–1699 (2000)
47. V. Puri, R. Watanabe, R.D. Singh, M. Dominguez, J.C. Brown, C.L. Wheatley, D.L. Marks, R.E. Pagano. Clathrin-dependent and -independent internalization of plasma membrane sphingolipids initiates two Golgi targeting pathways. *J Cell Biol*. 6, 154(3): 535–548 (2001)

48. I.R. Nabi, P.U. Le. Caveolae/raft-dependent endocytosis. *JCB*. 161, 4: 673–677 (2003)
49. R.G. Parton, M.A. Pozo. Caveolae as plasma membrane sensors, protectors and organizers. *Nature Reviews Molecular Cell Biology*. 14: 98–112 (2013)
50. J.P. Luzio, P.R. Pryor, N.A. Bright, Lysosomes: fusion and function. *Nature Reviews Molecular Cell Biology*. 8: 622–632 (2007)
51. A. Hayer, M. Stoeber, D. Ritz, S. Engel, H.H. Meyer, A. Helenius. Caveolin-1 is ubiquitinated and targeted to intraluminal vesicles in endolysosomes for degradation. *J Cell Biol*. 1, 191(3): 615–629 (2010)
52. H. Lodish, A. Berk, S. L. Zipursky, P. Matsudaira, D. Baltimore, J. Darnell, *Molecular Cell Biology*, 4th edition. Redaktorius: W. H. Freeman. New York, 2000
53. R. Dobrowolski, E.M. Robertis, Endocytic control of growth factor signalling: multivesicular bodies as signaling organelles. *Nat Rev Mol Cell Biol*. 23, 13 (1): 53–60 (2011)
54. P. Liu, M. Rudick, R.G.W. Anderson. Multiple functions of caveolin-1. *The Journal of Biological Chemistry*. 277: 41295–41298 (2002)
55. W.P. Li, P. Liu, B.K. Pilcher, R.G.W. Anderson. Cell-specific targeting of caveolin-1 to caveolae, secretory vesicles, cytoplasm or mitochondria. *J. Cell Sci*. 114: 1397–1408 (2001)
56. D.E.J.G.J. Dolmans, D. Fukumura, R.K. Jain. Photodynamic therapy for cancer. *Nature Reviews Cancer*. 3: 380–387 (2003)
57. K.A. Al-Khazaleh, K. Omar, M.S. Jaafar. pH effect on cellular uptake of Sn(IV) chlorine e6 dichloride trisodium salt by cancer cells in vitro. *Journal of Biological Physics*. 37, 1: 153–161 (2011)
58. H. Mojzisoava, S. Bonneau, C. Vever-Bizet, D. Brault. Cellular uptake and subcellular distribution of chlorin e6 as functions of pH and interactions with membranes and lipoproteins. *Biochimica et Biophysica Acta – Biomembranes*. 1768, 11: 2748–2756 (2007)
59. T. Boulikas, M. Vougiouka. Cisplatin and platinum drugs at the molecular level (Review). *Oncology Reports*. 10, 6: 1663–1682 (2003)
60. G. Ciarimboli. Membrane transporters as mediators of cisplatin effects and side effects. *Scientifica*. 2012: 473829 (2012)
61. J. Park, J. Nam, N. Won, H. Jin, S. Jung, S. Jung, S. H. Cho, S. Kim, Compact and stable quantum dots with positive, negative, or zwitterionic surface: specific cell interactions and non-specific adsorptions by the surface charges. *Advanced Functional Materials*. 21, 9: 1558–1566 (2011)
62. O. Harush-Frenkel, N. Debotton, S. Benita, Y. Itschuler. Targeting of nanoparticles to the clathrin-mediated endocytic pathway. *Biochemical and Biophysical Research Communications*. 353, 1: 26–32 (2007)

63. Y. Zhang, H. Pan, P. Zhang, N. Gao, Y. Lin, Z. Luo, P. Li, C. Wang, L. Liu, D. Pang, L. Cai, Y. Ma. Functionalized quantum dots induce proinflammatory responses in vitro: the role of terminal functional group-associated endocytic pathways. *Nanoscale*. 5: 5919–5929 (2013)
64. A. Andersson, H. Hedenmalm, B. Elfsson, H. Ehrsson. Determination of the acid dissociation constant for cis-diammineaquachloroplatinum(II) ion. A hydrolysis product of cisplatin. *Journal of Pharmaceutical Sciences*. 83, 6: 859–862 (1994)
65. S. Bhattacharjee, D. Ershov, J. Gucht, G. M. Alink, I. M. C. M. Rietjens, H. Zuilhof, A. T. M. Marcelis. Surface charge-specific cytotoxicity and cellular uptake of tri-block copolymer nanoparticles. *Nanotoxicology*. 7, 1: 71–84 (2013)
66. V. Karabanovas, R. Rotomskis, A. Beganskiene, A. Kareiva, S. Bagdonas, P. Grigaravicius, K.O. Greulich. Degradation Related Cytotoxicity Of Quantum Dots. 9th IEEE Conference on Nanotechnology (IEEE-NANO). 2009: 454-457 (2009)
67. U.E. Martinez-Outschoorn, D. Whitaker-Menezes, S. Pavlides, B. Chiavarina, G. Bonuccelli, C. Trimmer, A. Tsigirgos, G. Migneco, A.K. Witkiewicz, R. Balliet, I. Mercier, C. Wang, N. Flomenberg, A. Howell, Z. Lin, J. Caro, R.G. Pestell, F. Sotgia, M.P. Lisanti. The autophagic tumor stroma model of cancer or “battery-operated tumor growth” - a simple solution to the autophagy paradox. *Cell Cycle*. 9, 21: 4297–4306 (2010)
68. Y.H. Luo, S. Wu, Y. Wei, Y. Chen, M. Tsai, C. Ho, S. Lin, C. Yang, P. Lin. Cadmium-Based Quantum Dot Induced Autophagy formation for cell survival via oxidative stress. *Chem. Res. Toxicol.* 26, 5: 662–673 (2013)
69. W. Li, H. Liu, J. Zhou, J. Cao, X. Zhou, A. M. K. Choi, H. Shen, Z. Chen, Caveolin-1 inhibits expression of antioxidant enzymes through direct interaction with nuclear erythroid 2 p 45-related factor-2 (Nrf2). *The Journal of Biological Chemistry*. 287: 20922–20930 (2012)
70. A.M. Florea, D. Büsselberg. Cisplatin as an anti tumor drug: cellular mechanisms of activity, drug resistance and induced side effects. *Cancers*. 3, 1: 1351–1371 (2011)
71. B.A. Kairdolf, A.M. Smith, T.H. Stokes, M.D. Wang, A.N. Young, S. Nie. Semiconductor quantum dots for bioimaging and biodiagnostic applications. *Annu Rev Anal Chem*. 12, 6(1): 143–162 (2013)
72. A. Manke, L. Wang, Y. Rojanasakul. Mechanisms of nanoparticle-induced oxidative stress and toxicity. *BioMed Research International*. 2013: 942916 (2013)
73. M. Ahamed, H.A. Alhadlaq, J. Alam, M.A Khan, D. Ali, S. Alarafi. Iron oxide nanoparticle-induced oxidative stress and genotoxicity in human skin epithelial and lung epithelial cell lines. *Current Pharmaceutical Design*. 19, 37: 6681–6690 (2013)
74. S. Kim, D. Ryu. Silver nanoparticle-induced oxidative stress, genotoxicity and apoptosis in cultured cells and animal tissues. *Journal of Applied Toxicology*. 33, 2: 78–89 (2013)

75. H. Yang, C. Liu, D. Yang, H. Zhang, Z. Xi. Comparative study of cytotoxicity, oxidative stress and genotoxicity induced by four typical nanomaterials: the role of particle size, shape and composition. *Journal of Applied Toxicology*. 29, 1: 69–78 (2009)
76. P. Nativo, I.A. Prior, M. Brust. Uptake and intracellular fate of surface-modified gold nanoparticles. *ACS Nano*. 2, 8: 1639–1644 (2008)
77. J. Dausend, A. Musyanovych, M. Dass, P. Walther, H. Schrezenmeier, K. Landfester, V. Mailänder. Uptake mechanism of oppositely charged fluorescent nanoparticles in HeLa cells. *Macromolecular Bioscience*. 8, 12: 1135–1143 (2008)
78. N. Hao, L. Li, Q. Zhang, X. Huang, X. Meng, Y. Zhang, D. Chen, F. Tang, L. Li. The shape effect of PEGylated mesoporous silica nanoparticles on cellular uptake pathway in HeLa cells. *Microporous and Mesoporous Materials*. 162, 1: 14–23 (2012)
79. M. Moros, B. Hernáez, E. Garet, J.T. Dias, B. Sáez, V. Grazú, Á. González-Fernández, C. Alonso, J.M. de la Fuente. Monosaccharides versus PEG-functionalized NPs: influence in the cellular uptake. *ACS Nano*. 6, 2: 1565–1577 (2012)
80. E. Morales-Avila, G. Ferro-Flores, B.E. Ocampo-García, L.M. Gómez-Oliván. Engineered multifunctional RGD-gold nanoparticles for the detection of tumour specific expression: chemical characterisation and ecotoxicological risk assessment. *Journal of Biomedical Nanotechnology*. 8, 6: 991–999 (2012)
81. T.M. Allen. P.R. Cullis. Liposomal drug delivery systems: from concept to clinical applications. *Advanced Drug Delivery Reviews*. 65, 1: 36–48 (2013)
82. J.W. Park, K. Hong, D.B. Kirpotin, G. Colbern, R. Shalaby, J. Baselga, Y. Shao, U.B. Nielsen, J.D. Marks, D. Moore, D. Papahadjopoulos, C.C. Benz. Anti-HER2 immunoliposomes: enhanced efficacy attributable to targeted delivery, *Clin. Cancer Res*. 8: 1172–1181 (2002)
83. H. Chen, H. Paholak, M. Ito, K. Sansanaphongpricha, W. Qian, Y. Che, D. Sun. 'Living' PEGylation on gold nanoparticles to optimize cancer cell uptake by controlling targeting ligand and charge densities. *Nanotechnology*. 6, 24(35): 355101 (2013)
84. A. Lesniak, A. Salvati, M.J. Santos-Martinez, M.W. Radomski, K.A. Dawson, C. Åberg. Nanoparticle adhesion to the cell membrane and its effect on nanoparticle uptake efficiency. *J. Am. Chem. Soc*. 135, 4: 1438–1444 (2013)

6 Santrauka

6.1 Aktualumas

Per pastarąjį dešimtmetį nanotechnologijų taikymas medicinoje ir nanomedžiagų naudojimas vystant naujas vaistų formas (vienu žodžiu apibūdinamas kaip nanomedicina) tapo pagrindiniu inovacijų įkvėpimo šaltiniu kuriant naujus vaistų pernašos būdus, skirtus pagerinti veiksmingumo ir toksiškumo santykį bei įgalinti suasmenintą mediciną. Pagrindinis pernašai skirtų nanodalelių privalumas yra galimybė realizuoti kelias funkcijas, vienoje nanodalelėje apjungiant diagnostikai ir terapijai skirtus preparatus, t.y., vaistus, atpažinimo ligandus ir vaizdinimo žymenis, taip įgalinant tikslinį vaistų pristatymą bei šio proceso stebėseną ir kontrolę. Nanonešikliu gali būti bet koks koloidinis objektas (organinės ir neorganinės nanodalelės, pūslelės, liposomos, micelės ir tirpios atitinkamo dydžio makromolekulės), kurio dydis yra nuo kelių nanometrų iki kelių mikrometrų. Ypatingai daug tyrimų atliekama kuriant nanonešiklius, kuriuos sudaro lipidų, polimerų molekulės, anglies, neorganiniai nanokristalai ir įvairios kompozitinės medžiagos, – ne tik tam, kad ženkliai pagerinti dabartinių vaistų farmakokinetines savybes, bet ir tam, kad pernešti organizme naujo tipo veiksmingus priešvėžinius vaistus, naudojamus genų ir imunoterapijoje.

Nanodalelėmis pagrįsta vaistų pernaša (NVP) – tai būdas, kuriuo siekiama pagerinti esamų vaistų veiksmingumą bei sudaryti galimybes naujoms terapijos rūšims atsirasti. Daugelis atliktų mokslinių tyrimų parodė, kad NVP sinergiškai apjungia ir pagerina tokias skirtingas vaistų veiksmingumą lemiančias savybes, kaip pvz., mažesnis šalutinis poveikis, pailginta cirkuliacijos trukmė, kontroliuojamas dozavimas organizmo viduje bei tikslinis pristatymas. Tačiau tam, kad NVP būtų galima panaudoti klinikiniams taikymams, pvz., vėžinių susirgimų gydymui, reikalingos fundamentalios žinios ir įvairiapusis supratimas, kokį poveikį fizikocheminės nanodalelių savybės daro vaistų aktyvumui ir lemčiai biologinėse sistemose, *in vitro* ir *in vivo*.

Sisteminiam nanodalelėmis pagrįstos vaistų pernašos tyrimams reikalingos didelio jautrio, įgalinančios didelę skiriamąją gebą, kuo paprasčiau modifikuojamos bei nebrangios modelinės priemonės. Teoriškai, tokios priemonės turi išlaikyti originalių NVP nešiklių savybes ir elgseną biologinėje aplinkoje, tačiau įgalinti stebėti sisteminį ir viduląstelinį nanonešiklio patekimą į organizmą, pasiskirstymą jame, degradaciją,

veikliųjų medžiagų atpalaidavimą bei šalinimą. Puslaidininkiniai nanokristalai – kvantiniai taškai (KT) dėl savo unikalių fizikinių, cheminių ir optinių savybių, yra labai tinkamas modelis ir eksperimentinė platforma NVP procesų tyrimams, siekiant išmokyti kontroliuoti savybes, kuriomis turi pasižymėti nanonešikliai. KT vis daugiau dėmesio susilaukia dėl perspektyvų juos pritaikyti nanomedicinoje kaip diagnostikai ir gydymui skirtas priemonės, pavyzdžiui, atliekant tikslinį lokalių transformuotų ląstelių žymėjimą vėžio terapijoje. Be pagrindinių privalumų, pvz., didelės skiriamosios gebos įgalinimas, jautris aplinkos pokyčiams, plati spektrinio registravimo sritis, kurie atsiskleidžia panaudojant KT optiniam vaizdinimui, KT pasižymi mažu dydžiu, universaliomis paviršiaus cheminėmis bei išskirtinėmis optinėmis savybėmis – intensyvia FtL ir fotostabilumu, kurių dėka galima realaus laiko režimu stebėti ir registruoti jų elgseną biologinėse sistemose. Nepaisant to, kad KT dažniausiai yra sudaryti iš toksinių medžiagų, pvz., kadmio, tinkama danga pasyvuoti KT nesukelia ūmaus toksinio poveikio *in vitro* ir *in vivo*. KT savybės įgalino juos panaudoti modeliuojant įvairių nanodalelių tikslinio nutaikymo, patekimo į ląsteles ir transporto ląstelėse mechanizmus, bei šių tyrimų pagrindu siūlyti sprendimus, kaip reikėtų optimizuoti fizikochemines nanodalelių savybes ir paviršiaus junginių funkcionalumą specifiniams taikymams, ilgainiui kvantinį tašką pakeičiant kita, dominančia nanodalele, pvz., aukso nanodalele fototerminiai terapijai, bet nedarant poveikio jau nustatytoms nanonešiklio fizinėms savybėms ir lemčiai biologinėse sistemose.

Technologinė pažanga sintetinant vandeninėse terpėse suspenduojamus puslaidininkinius nanokristalus įgalino gaminti besiskiriančius dydžiu, paviršiaus aktyvumu, prijungiamomis prie paviršiaus biologinėmis molekulėmis ir tiksliai paskirtimi biosuderinamus kvantinius taškus. Nanodalelių dydis, krūvis, sudėtis ir cheminis aktyvumas (dangalo ir paviršiaus aktyvios grupės) yra laikomos ypatingai svarbiomis savybėmis, sąlygojančiomis nanodalelių sąveiką su biomolekulėmis ir biologinį atsaką, nes šių savybių pokyčiai ženkliai pakeičia nanodalelių patekimą į ląsteles, viduląstelinę lokalizaciją ir lemčių. Išsiaiškinus patekimo į ląsteles mechanizmus, kiekybiškai įvertinus nanodalelių patekimo į ląsteles spartą bei nustatčius jų lemčių ląstelės viduje, taptų įmanoma kontroliuoti pagrindinius veiksnius, apsprendžiančius klinikinius NVP naudojimo rezultatus. Yra atlikta daug ne vienoje apžvalgoje aprašytų tyrimų *in vitro* ir *in vivo*, kuriais siekiama atrasti sąsajas tarp šių KT savybių ir ląstelėse stebimų

biomolekulinių signalų, viduląstelinio transporto ir toksinio poveikio). Tačiau, remiantis dabartine mokslinėje literatūroje pateikiama informacija, yra sudėtinga padaryti apibendrinančias išvadas apie optimalias biomedicininio atžvilgiu nanodalelių savybes, nes tyrimų rezultatai aprėpia labai įvairias nanodaleles, gauti tiriant jas skirtingose ląstelių linijose ir taikant skirtingus metodus. Taip pat, dauguma skelbtų pradinių išvadų turi būti tikslinamos, remiantis naujomis žiniomis apie nanodalelių patekimo į ląsteles mechanizmus ir nuo to priklausančią jų lemtį. Todėl nanodalelių patekimo į ląsteles, viduląstelinio transporto ir pasiskirstymo dėsningumų ištyrimas leistų tiksliau interpretuoti duomenis gaunamus *in vitro* tyrimais ir pasitarnautų nanodalelių panaudojimo *in vivo* plėtrai.

6.2 Tyrimų tikslas ir uždaviniai

Tyrimų tikslas – naudojant kvantinius taškus, kaip tinkamų vaistų pernašai biosuderinamų nanodalelių modelį, *in vitro* nustatyti bendrus tikslingai nemodifikuotų nanodalelių patekimo į ląsteles ir lokalizacijos jose dėsningumus.

Tiksliui pasiekti buvo suformuluoti šie tyrimų uždaviniai:

1. Fluorescencinės spektroskopijos metodu išmatuoti kvantinių taškų kaupimosi ląstelėse laikinę dinamiką vėžinių ir nevėžinių ląstelių kultūrose.
2. Iširti viduląstelinį kvantinių taškų pasiskirstymą konfokalinės fluorescencinės mikroskopijos ir fluorescencijos gyvavimo trukmės vaizdinimo mikroskopijos metodais.
3. Nustatyti kvantinių taškų patekimo į ląsteles būdus ir juos sąlygojančius veiksnius.
4. Įvertinti kvantinių taškų, kaip diagnostinių priemonių, poveikį ląstelėms kombinuoto gydymo modelio atveju.

6.3 Ginamieji teiginiai

1. Tikslingai nemodifikuotų neigiamo apvalkalo krūvio kvantinių taškų (KT) patekimas į visų tirtųjų linijų ląsteles yra netiesinis procesas, vykstantis trimis, nors ir skirtingos trukmės, etapais: I – lėtuojų, II – augimo ir III – soties, o KT kaupimąsi, atsižvelgiant į pasiskirstymą ląstelėse, galima suskirstyti į keturias fazes: 1-oji – KT prikibimas prie membranos; 2-oji – vezikulinių struktūrų su KT

formavimas ir pasklidimas citoplazmoje; 3-oji – vezikulių su KT susiliejimas ir lokalizacija aplink branduolį; 4-oji – multivezikulinių kūnelių su KT formavimas ir pasiskirstymas citoplazmoje.

2. Kvantinius taškus sukaupusios endosomos patiria brandos pokyčius, formuojantis heterogeninėms vidinėms struktūroms, kuriose KT fotoluminescencijos gyvavimo trukmė trumpėja.
3. Kvantiniai taškai per ląstelės išorinę ar vidines membranas difuzijos būdu neprasiskverbia.
4. Kvantiniai taškai aplinkoje be serumo baltymų į fibroblastų ląsteles (NIH3T3) patenka tik vienu, su kaveolinu susijusios endocitozės būdu, kurį patys slopina, tačiau stebimas nuslopinimas yra laikinas.
5. Kvantinių taškų susikaupimas ląstelėse gali paveikti tiek vaistinių preparatų patekimą į ląsteles, tiek ir ląstelių atsparumą jiems.

6.4 Naujumas

Šio mokslinio darbo metu buvo pirmą kartą atlikti ir nuosekliai aprašyti išsamūs tikslingai nemodifikuotų neigiamą paviršiaus krūvį turinčių kvantinių taškų (KT) kaupimosi ląstelėse tyrimai, apimantys KT kaupimosi etapus, paskirstymą ląstelėse, susiformavusių endosomų struktūros analizę bei KT patekimo į ląsteles mechanizmo nustatymą.

Pirmą kartą ilgame laiko intervale buvo ištirti ir nustatyti laikiniai netikslinių KT kaupimosi etapai (I – lėtasis ($t_{ink} < 0,5$ val.), II – augimo ($t_{ink} 0,5-6$ val.) ir III – soties ($t_{ink} > 6$ val.)) bei KT pasiskirstymo ląstelėse fazės (1-oji fazė – prikibimas prie membranos ($t_{ink} 0,5-1$ val.), 2-oji fazė – vezikulinių struktūrų formavimas ir pasklidimas citoplazmoje ($t_{ink} 0,5-6$ val.), 3-oji fazė – vezikulių susiliejimas ir lokalizacija aplink branduolį ($t_{ink} 6-24$ val.) ir 4-oji fazė – multivezikulinių kūnelių formavimas ir pasiskirstymas citoplazmoje ($t_{ink} > 24$ val.)). Pirmą kartą parodyta, kad naudojant fluorescencijos gyvavimo trukmės vaizdinimo mikroskopijos (FLIM) metodiką, galima identifikuoti KT sukaupusias vezikules pagal jų brandą bei vizualizuoti vidines vezikulių struktūras.

Pirmą kartą buvo atlikta KT suspensijos mikroinjekcija į ląsteles, siekiant imituoti galimą nanodalelių difuziją per išorinę ląstelės membraną. Atlikus palyginamuosius KT

kaupimosi tyrimus ląstelėse po laikinosios transfekcijos su žaliai fluorescuojančio baltymo (EGFP) plazmide, buvo parodyta, kad KT difuziškai neprasiskverbia nei per išorinę, nei per vidines ląstelės membranas.

Buvo nustatyta, kad tikslingai nemodifikuoti neigiamo paviršiaus krūvio KT į NIH3T3 ląsteles patenka nuo kaveolino priklausančiu endocitozės būdu, bei pirmą kartą parodyta, kad įsisotinantis KT kaupimasis sąlygojo viduląstelinį kaveolino-1, kuris yra pagrindinė molekulė, reikalinga membranos įlenkimui ir kaveolino struktūrų formavimui, persiskirstymą ir susikaupimą KT pripildytose vezikulėse.

Taip pat buvo užregistruotas padidėjęs tirtų ląstelių atsparumas cisplatinos poveikiui dėl KT įsisotinčio kaupimosi, o tai yra labai svarbu siekiant toliau plėtoti KT pritaikomumą diagnostikos ir kombinuotos terapijos poreikiams.

6.5 Pagrindiniai rezultatai

Šiame darbe buvo atlikti nuoseklūs, apimantys ilgą laiko intervalą (0 – 48 val. ir 96 val.) kvantinių taškų patekimo į ląsteles tyrimai, kurie padėjo nustatyti ląstelėse vykstančius KT kaupimosi ir viduląstelinio pasiskirstymo pokyčius ir suformuluoti bendrus tikslingai nemodifikuotų nanodalelių patekimo į ląsteles ir lokalizacijos jose dėsningumus.

KT, dengtų neigiamo paviršinio krūvio karboksilo grupėmis kaupimosi ląstelėse eiga galima suskirstyti į tris pagrindinius etapus: lėtąjį, augimo ir soties. Atlikus KT kaupimosi tyrimus skirtingų ląstelių linijose, buvo nustatyta, kad tirtose ląstelėse KT kaupimasis vyksta tais pačiais etapais, nepriklausomai ar tirtosios ląstelės buvo vėžinės, tačiau kiekvienai ląstelių linijai etapų trukmė yra skirtinga. Analizuojant KT-ais pripildytų vezikulių viduląstelinio pasiskirstymo kitimą laike buvo nustatyta, kad kiekviename iš kaupimosi etapų dominuoja skirtingos KT kaupimosi fazės: prikibimas prie membranos; vezikulinių struktūrų formavimas ir pasklidimas citoplazmoje; vezikulių susilieėjimas ir lokalizacija aplink branduolį; ir multivezikulinių struktūrų formavimas ir pasiskirstymas citoplazmoje. Nepaisant skirtingų KT kaupimosi etapų trukmių, tikslingai nemodifikuotų neigiamo krūvio apvalkalo KT kaupimosi fazės, nors stebėtos ir skirtingu inkubacijos metu, pagal susiformavusių vezikulių tipus ir viduląstelinį vezikulių pasiskirstymą yra panašios visose tirtose ląstelių linijose.

Šie nuoseklūs KT patekimo į ląsteles tyrimai įgalino analizuoti ir palyginti tarpusavyje skirtingų tyrėjų pateikiamus rezultatus apie KT ir kitas nanodaleles ląstelėse.

Mokslinėje literatūroje yra aprašomi nanodalelių patekimo į ląsteles tyrimai ir analizuojantys galimybę, kad nanodalelės ląstelėse kaupiasi ne per receptoriais valdomus endocitozės ar fagocitozės kelius, bet tiesioginės difuzijos per membraną būdu. Dėl to buvo nuspręsta atlikti palyginamąjį KT patekimo į ląsteles ir pasiskirstymo po jas tyrimą, imituojant pasyvią difuziją – t.y., tiesiogiai suleidžiant KT į ląsteles. Šio tyrimo metu stebėta KT fotoluminescencija ląstelėse buvo visiškai kitokia, nei natūraliai patekusių KT – po mikroinjekcijos suleisti KT iškart tolygiai pasiskirstė per visą citoplazmą – patvirtino, kad KT difuziškai neprasiskverbia per ląstelės plazminę membraną (nei iš išorės į vidų, nei iš vidaus į išorę), bet patenka endocitozės būdu. Pastebėtas vykstantis KT užpildytų vezikulių persitvarkymas (vezikulių dydžio pokyčiai, multivezikulinių kūnelių formavimasis) paskatino detaliau ištirti KT pernašą ląstelėse, KT užpildytų vezikulių susiliejamą bei patikrinti galimybę, kad uždaryti vezikulėse KT vis dėlto išstrūksta į citozolį. Tam buvo pasirinktos žaliai fluorescuojančiu baltymu transfekuotos ląstelės, kurių pagalba buvo nustatyta, kad nėra pasyvios KT pernašos iš citozolio į endosomas, bei iš endosomų į citozolį.

Siekiant atskleisti molekulinį KT endocitozės mechanizmą, buvo tiriamas įsisotinamo KT kaupimosi poveikis endocitozės mechanizmui bei skirtingų endocitozės žymeklių patekimui į ląsteles. Tyrimai atskleidė, kad soties etape KT patekimas į ląsteles yra tuo labiau slopinamas, kuo daugiau KT jau yra susikaupusių ląstelėse, tačiau ilgainiui kaupimasis vėl atsistato. Eksperimentai su žymekliais parodė, kad KT neturi ženklaus slopinamo poveikio transferino (nuo klatrino priklausančios endocitozės žymeklio) ir dekstrano (makropinocitozės substrato) patekimui į ląsteles. Tačiau, laktozilceramido (kaveolino ligando, į žinduolių ląsteles selektyviai patenkantis kaveolino reguliuojamu keliu) kaupimasis buvo beveik pilnai sutrikdytas KT prisotintose ląstelėse. Taip pat buvo nustatyta, kad kaupiantis KT, kai jie patenka į ląsteles nuo kaveolino priklausančiu endocitozės būdu, normali kaveolino-1 apykaita sutrikdoma dėl sąveikos tarp KT ir kaveolino ir tai sąlygoja kaveolino-1 persiskirstymą nuo ląstelės išorinės membranos į endosomas.

Atlikti KT kaupimosi ląstelėse tyrimai parodė, kad KT biomediciniuose taikymuose neturėtų būti laikomi paprastais zondais, žymekliais ar nešėjais, nes jie taip pat sąlygoja

ir įvairius biologinius efektus. Dėl to, siekiant praplėsti žinias, kurios padėtų įvertinti naujų kombinuotos terapijos metodų sukūrimo ir teranostinio KT panaudojimo galimybes, buvo atlikti *in vitro* tyrimai vertinant KT suderinamumą su kitais terapijoje naudojamais preparatais. Tyrimams buvo pasirinkti fotosensibilizatorius chlorinas e6, plačiai taikomas fotodinaminėje vėžinių susirgimų terapijoje, ir cisplatina, kuri yra plačiai naudojama kaip priešvėžinis vaistas. KT kaupimasis ląstelėse neturėjo poveikio chlorino e6 susikaupimui, tačiau sąlygojo didesnę ląstelių atsparumą cisplatinos chemotoksiniam poveikiui. Šį KT poveikį ląstelėms būtina įvertinti prieš naudojant kvantinius taškus ir kitas nanodaleles kombinuotoje diagnostikoje ir terapijoje *in vivo*.

6.6 Išvados

1. Spektroskopiniais metodais ištyrus kvantinių taškų patekimo į ląsteles laikinę dinamiką nustatyta, kad neigiamo krūvio apvalkalo kvantinių taškų patekimo į ląsteles procesą galima suskirstyti į tris etapus: I – lėtąjį, II – augimo ir III – soties, kurie yra būdingi tirtoms vėžinių MCF-7, HepG2 ir nevėžinių NIH3T3 ląstelių linijoms. Tačiau šie kaupimosi etapai skirtingose ląstelių kultūrose yra nevienodos trukmės.
2. Konfokalinės fluorescencijos mikroskopijos metodu ištyrus neigiamo paviršiaus krūvio kvantinių taškų patekimo į ląsteles procesą, pagal viduląstelinį kvantinių taškų pasiskirstymą ir susiformavusių pūslelių tipus, galima suskirstyti į keturias fazes: 1-oji fazė – prikibimas prie membranos; 2-oji fazė – vezikulinių struktūrų formavimas ir pasklidimas citoplazmoje; 3-oji fazė – vezikulių susilieėjimas ir lokalizacija aplink branduolį; 4-oji fazė – multivezikulinių kūnelių formavimas ir pasiskirstymas citoplazmoje.
3. Naudojant fluorescencijos gyvavimo trukmės vaizdinimo mikroskopijos metodą užregistruotas nuo endosomų brandos priklausantis viduląstelinis vezikulių vidinės struktūros heterogeniškumas. Skirtingos brandos endosomos gali būti apibūdinamos ir vaizdinamos remiantis jose sukauptų kvantinių taškų savitomis fotoluminescencijos gyvavimo trukmėmis (endocitotinės vezikulės – 16-22 ns, ankstyvosios endosomos – 10-15 ns, ir vėlyvosios endosomos bei multivezikuliniai kūnai – 5-9 ns).

4. Skirtingais fizikiniais ir biocheminiais metodais nustatyta, kad difuzijos būdu kvantiniai taškai per ląstelės membraną neprasiskverbia, bet į ląsteles patenka endocitozės būdu. Kvantinių taškų patekimo kelią keičia jų paviršiuje susiformuojantis baltymų vainikas. Nepadengti baltymais neigiamo paviršiaus krūvio kvantiniai taškai į ląsteles patenka tik vienu nuo kaveolino priklausančiu endocitozės keliu.
5. Kvantinių taškų, kaip modelinių diagnostinių priemonių, ir antivežinio preparato cisplatinos bendras panaudojimas *in vitro* atskleidė, kad kvantiniai taškai, nesukeldami toksinio poveikio ląstelių gyvybingumui ir dalijimuisi, padidino ląstelių atsparumą. Tokio pobūdžio sąveikas būtina įvertinti prieš naudojant nanodaleles su vaistiniais preparatais kombinuotoje diagnostikoje ir terapijoje *in vivo*.

7 List of publications

Publications in peer-reviewed journals:

- L. Damalakiene, V. Karabanovas, S. Bagdonas, L. Pupelis, M. Valius, R. Rotomskis. Suppression of a Specific Intracellular Uptake Pathway by a Saturating Accumulation of Quantum Dots. *Journal of Biomedical Nanotechnology*. (Accepted for publication, 2015);
- L. Damalakiene, V. Karabanovas, S. Bagdonas, M. Valius, R. Rotomskis. Intracellular distribution of non-targeted quantum dots after natural uptake and microinjection. *International Journal of Nanomedicine*, 8(1): 555 – 568, 2013.

Conference proceedings:

- L. Damalakiene, S. Bagdonas, R. Rotomskis, V. Karabanovas, M. Ger, M. Valius. Influence of growth factor on internalization pathway of quantum dots into cells: PDGF effects internalization of QDs. 9th IEEE Conference on Nanotechnology (IEEE-NANO), 465 – 468, 2009, July 26-30, Genoa, Italy.

National and international conferences:

- L. Damalakiene. Cluster Lithuanian Plastic and Novel Materials Cluster: activities in the area of nano-bio interface. 2nd International Conference on Biomaterials Science – ISBC2013. 19-22nd of March, 2013, Tsukuba, Japan.
- L. Damalakiene, S. Bagdonas, R. Rotomskis, M. Ger, M. Valius. Accumulation of quantum dots in different cell lines. *Nanotech Europe 2009*. 28-30th of September, 2009, Berlin, Germany.
- L. Bandzaityte, M. Ger, T. Daunoravičius, V. Karabanovas, S. Bagdonas, M. Valius, R. Rotomskis. Accumulation and distribution of quantum dots in cell cultures. International conference "Innovative methods and technologies in biomedicine". 22-24th of May, 2009, Vilnius, Lithuania.
- L. Bandzaitytė, S. Bagdonas, R. Rotomskis, Z. Žitkus, M. Valius. Influence of growth factor on accumulation of quantum dots in cells. 7th ScanBalt Forum and Biomaterials Days 2008. 24-26th of September, 2008, Vilnius, Lithuania.

8 CURRICULUM VITAE

Personal information

First name / Surname **Leona Damalakiene (Bandzaityte)**
Address Zirgo 1-26, 10221, Vilnius, Lithuania
Telephone Mobile: +370 686 14280
E-mail leona.bandzaityte@gmail.com
Nationality Lithuanian
Date of birth 1980-06-26

Education

Dates 2006 – 2014
Title of qualification PhD student
Principal subjects Biomedical applications, nanomedicine, nanotechnology
Name and type of organisation
providing education and training Faculty of Physics, Vilnius University
Dates 2002 - 2004
Title of qualification awarded MSc
Principal subject Biophysics
Name and type of organisation
providing education and training Faculty of Physics, Vilnius University
Dates 1998 - 2002
Title of qualification awarded BSc
Principal subject Management of modern technologies
Name and type of organisation
providing education and training Faculty of Physics, Vilnius University

Work experience

Dates 2014 - present
Position Project Manager
Main activities and responsibilities Team management, technology/innovation facilitation, project management.
Name and address of employer UAB “Advanced Advice”, Vilnius str. 35, Vilnius LT-01119, Lithuania

Dates	2002 - 2014
Position held	Project Manager, Partner
Main activities and responsibilities	<p>2012 - 2014: Partner with additional activity – strategic business planning (inc. development of operational and financial models);</p> <p>2010 - 2014: Project Manager: technology/innovation facilitation, project management, proposal writing, preparation of foresight, feasibility studies and business plans and organisation of workshops, preparation of teaching materials and giving lectures on project and/or innovation management.</p> <p>2006 - 2010: Project Manager with main activities of proposal writing and project management.</p> <p>2002 – 2006: Project Manager with main activities of idea screening, proposal writing and administrative management.</p>
Name and address of employer	UAB “Europarama”, Sauletekio av. 15, Vilnius LT-10224, Lithuania.
Type of business or sector	Consultancy
Additional information	
Interests	Nanomedicine, theranostics, biomedical imaging, biotechnology, nanotechnology, technology transfer and business development.
Expert evaluator	Since 2008: Expert evaluator subcontracted by European Commission for proposal evaluation of Framework programme Marie Curie International Training networks (2008, 2010, 2011, 2012); Erasmus Mundus Master and PhD programmes (2012); Tempus IV (2013); Horizon2020 (2014).
Proposal and study writing	<ul style="list-style-type: none"> - Proposals for Horizon2020, FP7 and FP6: 7 in total (successful out of 12); - More than 10 proposals for funding form ERDF; - Feasibility studies (themes: nanotechnology, biotechnology, renewable resources, laser application, different engineering solutions, more than 10); - Visions and Strategies for development of national industrial clusters and associations (4); - Business plans for innovative products (more than 10); - Contribution to preparation of 2 Foresight studies on research development and development particular industrial sector in Lithuania.

Project management and implementation

- SMART-*FLeX*: Demonstration at industrial scale of the *FLeX*ible manufacturing of SMART multifunctional photovoltaic building elements. FP7 Collaborative project, Grant Agreement no.: ENER/FP7/322449/SMART-*FLeX* (2013-2016, 8 partners from 4 countries, budget 4,8 M€). Role: proposal writing, negotiation and overall project management;
- SOLGAIN: Competitive stationary low concentrating solar module of novel design. FP7 Research for SMEs, Grant Agreement no.: 315663 (2012-2014, 8 partners from 5 countries, budget: 1,5 M€). Role: proposal writing, negotiation and overall project management;
- PV4B: Photovoltaic technologies for business. ERDF project, Contract no.: VP2-1.4-ŪM-01-K-01-002 (2010-2013, single partner, budget: 0,8 M€). Role: proposal writing, negotiation, overall project management and implementation of project tasks;
- OPENPLAST: Development of Cluster of Plastic and Novel Materials. ERDF project, Contract no.: VP2-1.4-ŪM-01-K-01-032 (2012-2014, single partner, budget: 100 k€). Role: implementation of project tasks;
- NANOPLASTAS: Development of next generation thermo isolation material with embedded nanoparticles Contract no.: VP2-1.3-ŪM-02-K-02-079 (2011-2014, 2 partners from 1 country, budget: 0,5 M€). Role: overall project management;
- MULTINANO: Multifunctional nanoparticles for specific non-invasive early diagnostics and treatment of cancer. Norwegian Financial Mechanism and Republic of Lithuania, Contract no.: LT0036 (2008-2010, 2 Lithuanian partners, budget 250 k€). Role: proposal writing, negotiation, project management and implementation of project tasks relevant to my PhD studies.;
- BALICTIME: Reinforcing eGovernment services in Baltic States through legal and accountable Digital Time Stamp. FP6 project, Contract no.: 027751 (2007-2010, 8 partners from 5 countries, budget: 1,5 M€). Role: proposal writing, negotiation and overall project management;
- PURILEACH: Modular purification system for heavily polluted leachate, FP6 project, Contract no.: 508698 (2004-2006, 11 partners from 5 countries, budget: 0,7 M€). Role: proposal writing, negotiation and administrative project management;

	<ul style="list-style-type: none"> - ULSYS: Multi monitoring medical chip for homecare applications, FP6 project, Contract no.: 508739 (2004-2006, 10 partners from 4 countries, budget: 1 M€). Role: negotiation and administrative project management; - NENNET: High Quality Research Network on Nanosciences, Material and Energy research in Lithuania. FP6 Support Action project, Contract no.: 510366 (2004-2006, 8 partners from 4 countries, budget: 200 k€). Role: assistance in project management, implementation of project tasks; - More than 10 short, single partner projects dedicated to preparation steps of innovative product development and commercialization.
Recent participation in conferences:	Vilnius Innovation Forum 2013 "Innovation Drift" (Vilnius, Lithuania), MANUFUTURE 2013 Conference (Vilnius, Lithuania), Conference on Biomaterials Science – ISBC2013 (Tsukuba, Japan), Bio-Europe Spring 2013 (Barcelona, Spain), BioInterface Conference 2012 (Dublin, Ireland)
Certificates	“Cost-Benefit Analysis for EU Projects” (European Academy for Taxes, Economics & Law, 2009, Berlin)